
Multistability and Transient Dynamics on Networked Systems

Der Fakultät für Mathematik & Naturwissenschaften
der Carl von Ossietzky Universität Oldenburg
zur Erlangung des Grades und Titels
Doktor der Naturwissenschaften (Dr. rer. nat.)
angenommene Dissertation

von

Kalel Luiz Rossi

geboren am 13.10.1997 in Curitiba, Parana, Brasilien

Gutachter: Prof. Dr. Ulrike Feudel

Gutachter: Prof. Dr. Klaus Lehnertz

Tag der Disputation: 15.01.2024

Contents

List of Publications	4
Abstract	5
Zusammenfassung	6
1 Introduction	7
2 Methodology	13
2.1 Some fundamental aspects of dynamical systems theory	13
2.1.1 Our dynamical systems and the uniqueness and existence of their solutions	13
2.1.2 The fate of linear dynamical systems	13
2.1.3 The fate of nonlinear dynamical systems I: attractors	14
2.1.4 Formalizing attractors and basins	16
2.1.5 Invariant manifolds: structures that organize state space	17
2.1.6 The fate of nonlinear dynamical systems II: multistability and basins of attraction	19
2.1.7 How to find attractors	21
2.2 Bifurcations	22
2.2.1 Saddle-node bifurcation of equilibria	22
2.2.2 Hopf bifurcation	23
2.2.3 Homoclinic bifurcation	24
2.3 Basics of network theory	24
2.4 Basics of Kuramoto oscillators	26
2.4.1 Derivation of the model and transition to synchronization	26
2.4.2 Multistability in homogeneous case: twisted states	28
3 Conclusions	31

List of Publications

This dissertation is based on the following publications:

Chapter 3: Kalel L. Rossi, Roberto C. Budzinski, Bruno R. R. Boaretto, Lyle E. Muller, and Ulrike Feudel. Small changes at single nodes can shift global network dynamics. *Physical Review Research* 5, 013220 (2023).

Chapter 4: Kalel L. Rossi, Everton S. Medeiros, Peter Ashwin and Ulrike Feudel. Transients versus network interactions.

Chapter 5: Kalel L. Rossi, Roberto C. Budzinski, Bruno R. R. Boaretto, Lyle E. Muller, and Ulrike Feudel. Dynamical properties and mechanisms of metastability: a perspective in neuroscience.

On top of these main thesis papers, I have also collaborated in other works, which resulted in three further publications, with me as a co-author.

- George Datseris, Kalel L. Rossi, and Alexandre Wagemakers. Framework for global stability analysis of dynamical systems. *Chaos* 33, 073151 (2023).
- Bruno R. R. Boaretto, Roberto C. Budzinski, Kalel L. Rossi, Thiago L. Prado, Sergio R. Lopes and Cristina Masoller. Temporal Correlations in Time Series Using Permutation Entropy, Ordinal Probabilities and Machine Learning. *Entropy* 23, 1025 (2021).
- Bruno R.R. Boaretto, Roberto C. Budzinski, Kalel L. Rossi, Cristina Masoller, Elbert E.N. Macau. Spatial permutation entropy distinguishes resting brain states. *Chaos, Solitons and Fractals* 171, 113453 (2023).

Abstract

Zusammenfassung

Chapter 1

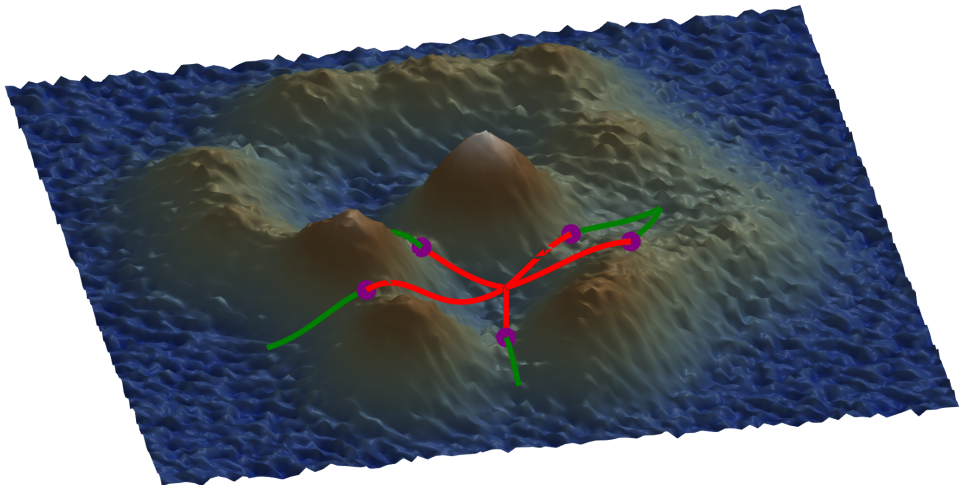
Introduction

Consider the unfortunate situation of falling down a mountain. Subject to the inexorable effect of gravity and friction, the hiker will roll downhill until they reach a certain valley, a spot at which they will finally terminate their unlucky dynamics. This final state is called an attractor. Now, consider a landscape like the one in Fig. 1.1A. The mountain here has several valleys, separated by peaks. An example of this is shown in Fig. 1.1B. Consider then the even more unfortunate situation of *two* people falling down a mountain. If they start very close together, on the same side of a peak, they will fall down to the same valley. If, however, they were separated by a peak when the fall started, then they will fall into distinct valleys. This is shown by the green and red trajectories in Fig. 1.1. Again, each valley is an attractor. An attractor is chosen by the initial condition - where the person was and how fast they were moving when they started to fall. All initial conditions that lead to the same attractor form a set called the basin of attraction of that attractor. All the red trajectories in Fig. 1.1A belong to the same basin. Trajectories are typically separated by peaks in the landscape (green and red of Fig. 1.1B), so the peaks usually form the boundaries between basins of attraction.

The example of the hiking disaster serves as a good introduction to the notion of *multistability* - the simultaneous coexistence of different ending states, different attractors, in a dynamical system with constant parameters (notice that the mountain landscape does not change in time in the example!). This phenomenon is present in a wide variety of notable systems, with potentially important real-world consequences [14, 47, 46]. In cells, multistability can explain how genetically identical cells can exist in multiple metabolically distinct stable states [71, 49]. Similarly, there has been evidence, and models, suggesting that multistability in the gut microbiome can explain microbiome shifts, changes in the composition of the microbiome in the gut [33]. On a technological side, power grids, networks of connected generators and consumers of electrical energy, need to operate on an attractor in which all units have their frequencies synchronized in the 50-60Hz range [25]. Multistability there is dangerous, as perturbations can switch the system out of the operating state, potentially leading to blackouts. Studies on models try to look for conditions that make the desired state as stable as possible [25, 24]. Multistability can also be a powerful mechanism in brain dynamics. Some models for long-term memory consider that each memory corresponds to an attractor in the system [68, 17]. Models of large-scale brain dynamics exhibit multistability [22]. There are many more examples, such as in artificial neural networks [16], models for ice sheets [50], mechanical systems [15], and in tissue repair [2].

The examples in neural networks and power grids in particular highlight the ubiquitous presence of multistability in networked systems - systems formed by the interactions of smaller subunits, such as neurons or electric generators. Another phenomenon in networks that can coexist with multistability is synchronization [45, 4]. In a synchronized network, the different subunits have similar activity - for instance, frequency synchronization occurs when individual oscillators with different natural frequencies spontaneously lock into a common frequency [60]. A perhaps more technically relevant example occurs has been mentioned before for power grids, in which all the units must have their frequencies synchronized at the same level, such as 50 Hz [25]. When units have the same frequencies and the phases of their oscillations are also the same,

A



B

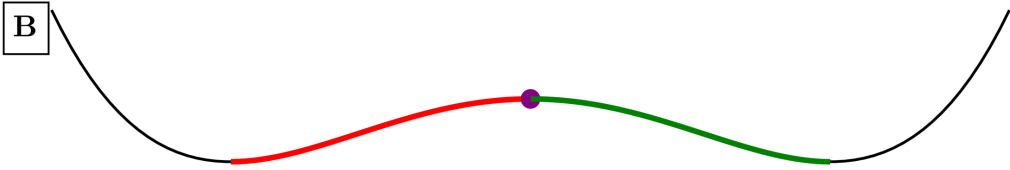


Figure 1.1: **Landscape with valleys and peaks constitutes an example of multistability for an unfortunate falling person.** Panels A and B respectively show a 3D and 2D example of a landscape, with red trajectories converging onto the same attracting region, and green trajectories, which start next to the red trajectories but on the other side of the peak, converge onto other attracting regions.

we talk of phase synchronization. This has also been proposed as an important mechanism in brain circuits [56, 18, 69]. Interestingly, lack of phase synchrony can also play an important role, e.g. in the flight pattern of fruit flies [29].

The real-world relevance of such systems has stimulated a lot of research into their dynamics [14]. An approach taken by several works has been to study simple models that capture some essential properties of real world systems. A particularly important example, which has become paradigmatic in the synchronization literature, is that of Kuramoto oscillators (see Sec.2.4). They constitute quite a beautiful example of how units with very simple dynamics can generate complex behavior when interacting together. Each unit in the model is described by a phase (angle) variable that by itself just varies linearly according to its own natural frequency. The interesting dynamics comes from the nonlinear coupling, done via the sin of the phase difference between coupled units, cf. (2.34). The model is simple enough to allow for analytic treatment but still complex enough to show relevant dynamics [60, 1]. In particular, it displays a continuous phase transition from desynchronization to frequency and phase synchronization as the strength of the inter-unit coupling is increased. Roughly, if the natural frequencies are spread too widely compared to the coupling between them, the units oscillate incoherently; if instead the coupling becomes large enough, the units start to oscillate with the same frequency - they become phase-

locked. As the coupling increases, the phases also become more clustered together, although complete phase synchronization does not occur.

The Kuramoto model is also generic in the sense that it can be derived as an approximation of general limit cycle oscillators under weak coupling [4]. In this case, one considers units that oscillate on a periodic orbit. If the coupling between the units is weak enough, the amplitude of their oscillation is not significantly affected, only the phase along the limit cycle. Then, the interplay between the differences in frequency and the coupling determines the time evolution of the phases. The Kuramoto model is a somewhat more specific case of this phase reduction, in that one chooses a purely sinusoidal coupling [60]. Still, the combination of simplicity and complexity leading to a synchronization transition, and this argument of genericity, incited a lot of research and inspired new concepts [1, 51, 60].

This also inspired us to translate results we had from spiking neural networks [7]. In those networks we described a phenomenon we called *dynamical malleability*, the sensitivity of a whole network's dynamics to changes in parameters of single components, usually changes in parameters of single units. Similarly to the Kuramoto oscillator networks, the spiking neural networks we studied also presented a transition to synchronization, in particular to phase synchronization, when the coupling strength was increased. They also presented a transition to synchronization as the topology changed: as the connections in the system are changed from being restricted only to k -nearest neighbors to being randomly allocated, the neurons also started to synchronize their phases. Types of topologies are better described in Sec. 2.3. In the neighborhood of both of these transitions, we showed that the network's dynamical malleability increased considerably. As we see in Chap. ??, this phenomenology generalizes for Kuramoto networks with heterogeneous frequencies. In fact, it occurs very strongly: changing the parameter of a single unit can drastically alter the behavior of the whole network in a very sensitive manner [53], which was until then not known.

In the literature for Kuramoto oscillators we found some works related to this. In a series of papers, Hong and colleagues studied this phenomenon from the point of view of statistical mechanics [27, 28], where dynamical malleability is often called sample-to-sample (STS) fluctuations. There, they say that the STS fluctuations increase near a phase transition. Changing the parameters of a single unit leads to a different network, which is termed to be a different sample. In this case, one shows that the finite size of the networks leads only to an approximate phase transition, whose critical parameter varies depending on the sample. These studies, however, did not look closely at the dynamics of these finite networks. One work that looks at this more closely for all-to-all topologies was Ref. [44], where they propose that the kurtosis of the natural frequency distribution correlates with the critical coupling strength of the transition - so changing frequency of units changes the kurtosis and thus changes this critical coupling strength. However, they did not explore how this also interacted with more complex topologies. As we then showed in our work, their mechanism alone does not explain the malleability we describe. One can compare networks with shuffled natural frequencies, which keeps the kurtosis constant, but still leads to high malleability. This malleability does come in part from the sample-to-sample fluctuations described for instance in works by Hong et al. [27]. But it also comes from multistability, which is another behavior we then analyzed.

We looked at multistability in the networks as a function of the coupling strength and topology, and showed the emergence of a large number of coexisting attractors at the transition to phase synchronization. This therefore means that the networks we studied are very sensitive to perturbations, in both the state variables (which can lead the system to switch to other attractors, due to multistability), or in the parameters (which can change the attractor considerably, due to malleability). This was another contribution from our work. Naturally, there have been studies on multistability in Kuramoto networks. In the case of heterogeneous frequencies, Tilles et al. studied multistability arising in nearest-neighbor rings [63]. In a related Kuramoto model, which as an inertial term, some studies have shown the coexistence of multiple attractors in random topologies [20], and in power grid topologies [25, 24]. Ref. [48] looks at how properties of power grid topologies relate to the dynamics of first-order Kuramoto models, but do not report multistability.

Multistability has been studied in detail for units with homogeneous frequencies (which are

then identical) and which are coupled in k -nearest-neighbor topologies. In this case, the network can be written as a gradient system, meaning its only attractors are equilibria, which are single points in state space (cf., Secs. 2.1.2-2.1.3). This considerably simplifies their study. The networks can have multiple stable equilibria, each being characterized by neighboring units having a fixed and constant phase relationship. These equilibria are called twisted states [67], and their stability depends on the relationship between the number of nearest neighbors k and the size N of the network [67] - see Sec. 2.4.2 for more.

For these networks there have been studies looking at the effect of the topology [65]. Another important contribution has looked at the basins of attraction for these networks. Zhang and Strogatz have shown that the basins behave like octopuses - the head of the octopus contains the attractor, an equilibrium. The head is relatively small compared to the tentacles: most of the volume of the basins is not concentrated around the equilibrium, but spread around in tentacle-like structures in state space [70].

In both the case of heterogeneous and of homogeneous frequencies, we are unaware of any systematic study on the emergence of multistability and effect of changing topology, in particular for first-order Kuramoto models. Inspired by this, we have started to study more deeply how exactly these attractors emerge and how their basins behave. This is subject for future work, but its basis is found in our study on malleability. In general, therefore, our work served to bridge two gaps in the Kuramoto literature: the dynamics of malleability and that of multistability, both of which contribute to understanding the sensitivity of this networks.

The mechanisms that give rise to multistability in networks in general are still not fully understood. In particular, during my PhD we started to study multistability in a network of bursting neurons coupled diffusively, looking to explain results from previous publications [52]. The neurons, which follow the Hindmarsh-Rose equations [26], have individually a stable periodic orbit as an attractor. By changing parameters of the neurons, one can make a certain region of this periodic orbit very slow, but without going through a bifurcation. Preliminary results showed that multistability only emerges in the coupled networks when the neurons have this slow region. To better understand this, we looked at a simpler conductance-based neuronal model [30] which also has regions of slow flow. We focused on the case when this model has excitable dynamics. The isolated neuron then has only one attractor, a stable equilibrium. And it also has two unstable equilibria, which force some trajectories to go on long excursions before converging to that attractor. These excursions are called excitations, and correspond to the neuron spiking. One of these unstable equilibria also slow down trajectories passing near it. By coupling two such neurons diffusively (Eq. ??) we show the emergence of different types of oscillating attractors, which can all coexist. We show the bifurcations giving rise to these attractors (more in Sec. 2.2). Further, we describe a qualitative mechanism for how they occur. The idea is that the diffusive coupling acts to repeatedly reinjecting the trajectories of each neuron into the region responsible for the excitations, thereby effectively *trapping the trajectories in this previously transient region* - see Chap. ?? for more. The slowness near one the equilibria plays an important role in this mechanism, which might help to explain the original problem we started on. For two units, it can happen that both are trapped in this excitability region, or just one is, generating in total three possible combinations. For more units, the number of possible combinations increases, and therefore so does the number of coexisting attractors. The emerging attractors are all oscillating, and can do so periodically, quasiperiodically, or chaotically - all despite the individual units having only equilibria! This mechanism is also a simple example of how coupling can interact with transients to generate attractors, an idea that has been studied in the literature under different circumstances. In particular, Medeiros et al. studied units which have a periodic attractor and a chaotic saddle, an unstable chaotic set, in their state space. They showed that diffusive coupling between them can counteract the divergence tendency near the chaotic saddle, effectively trapping the units in its neighborhood, and creating a chaotic attractor which coexists with the units' periodic attractor [39, 40]. However, the authors did not observe multiple attractors emerging from the trapping in the chaotic saddle. Therefore, the coupled excitable neurons, with their trapping mechanism, constitutes a simple yet powerful mechanism for generating a rich multistability in networks, which had not been described previously in the literature, to our knowledge.

This line of investigation on multistability also contributes to the study of how oscillations arise in non-oscillating units interacting via diffusive coupling. As discussed in Chap. ??, this line of work has a rich history, with an early work by Smale showing that Hopf bifurcations can give rise to oscillations [57] - see Sec. 2.2 for bifurcations. Later works showed the possibility of chaos, and also the emergence of multistability in repulsive coupling. Our contribution in this case has been to show a rich multistability, with the possible coexistence of periodic, quasiperiodic, and also chaotic solutions - with repulsive or attracting coupling.

These studies on multistability require efficient and reliable algorithms to identify the co-existing attractors of a system. To this end, I have contributed to creating `Attractors.jl`, an open-source package in the Julia programming language that collects such algorithms. In particular, George Datseris and Alexander Wagemakers had already introduced an algorithm to find attractors based on recurrences in state space [12], based on an idea by Nusse and Yorke [43]. I then contributed to implementing and refining another algorithm, proposed in Refs. [58, 20], based on finding attractors by grouping trajectories with similar features. These algorithms are described more in Sec. 2.1.7. Together with Datseris and Wagemakers, we built a continuation framework that allows one to use either of these two methods across a parameter range. This idea is similar to linear continuation analysis, but generalizes to any type of attractor, including chaotic attractors. This led to a publication [11]. On top of the novelty of the continuation algorithm, and the improvements made to the state of the art algorithms for finding attractors, our contribution here was also to provide a package that is free and easy to use.

If we think again about the excitable neurons, the multistability seen there is remarkable because stable states arise from the interaction with transient behavior (the excitations). Often in the literature we are preoccupied with the final states of the system - usually justifiably so - but anyone who asks the falling hikers in our initial example will probably find out that transients should not be disregarded so easily. In particular for neuroscience, transient dynamics has been the object of a lot of recent work. For instance, transients can be harnessed to perform computations [8], particularly when they are long-lived [35]. Ref. [35] proposes that long-lived transients, particularly in the form of ghosts of saddle-node bifurcations, offer some distinct computational advantages, such as maintaining a dynamical memory of a signal. See Sec. 2.2 for more on ghosts. For instance, Ref. [42] studied a simple model for how cells respond to changing chemical signals and use them to move. Without any signal, the cell operates on a stable equilibrium. A signal causes a saddle-node bifurcation that leads it to another stable equilibrium. As the signal is removed, the inverse bifurcation happens, and the cell eventually converges back to the original equilibrium. But before returning, the cell stays for a while visiting the ghost of the second equilibrium. Biologically, this means that cell keeps the memory of the signal for a while [42, 35]. Indeed, long-lived transients are an ubiquitous phenomenon observed in neural activity [64, 5], and are often referred to *metastability* there. One interesting example comes from studies measuring how mice encode for tastants fed to them. The study measured the firing rate activity in the gustatory cortex of the mice as a response to different tastants [31]. They identified that the stimulus elicits a sequence of distinct long-lived but transient regimes. By regime here we mean an epoch of the time series with some unique properties - in their case, the configuration of the average firing rate across the ensemble of neurons. Each tastant evoked a specific sequence of such metastable regimes. The duration of these regimes varies across trials, but the sequence itself is consistent [10, 5].

Delving into the metastability literature, we found that a general conceptual framework was lacking. First, the very definition of metastability varied between works, leading to apparent inconsistencies, as explained in more details in Chap. ???. Second, the mechanisms proposed for metastability also varied. Some works propose ghost of saddle-node bifurcations [64] while others propose noise [5], with few works attempting to compare different proposals [23]. In our work, we drew from tools of dynamical systems theory to provide such a conceptual framework. We provide a simple definition of metastable regimes as long-lived transients, which encompasses the majority of previous works not only in neuroscience, but also dynamical systems and even ecology. Previous inconsistencies between works can be neatly fit into distinct subtypes of metastability - for instance, when transitions between metastable regimes are spontaneously or externally driven. Then we use this definition to study general properties of metastability,

making use of the concept of almost-invariant sets [13, 19]. We also propose several dynamical mechanisms that can generate metastable regimes. Importantly, we connect these mechanisms to what had been proposed previously in the literature, gathering insights from different literatures.

Taking all of this together, my PhD has been a journey into studying the long-term and the transient dynamics of networked systems - how multistability can emerge and how it affects their robustness - and how long transients (metastability) can arise. This thesis describes this journey and will hopefully reflect the excitement of doing all of this research. In Chap. 2 I introduce in greater depth the fundamental concepts needed for the studies performed in this thesis. These will then follow in Chaps. ??, ?? and ?? in the same order introduced here. Finally, in Chap. 3 I will take all of these results together and reflect on what we learned, what our contributions have been to the literature, and the open questions that lie ahead in the future.

Chapter 2

Methodology

2.1 Some fundamental aspects of dynamical systems theory

2.1.1 Our dynamical systems and the uniqueness and existence of their solutions

In this thesis we study dynamical systems described by a state variable $x = (x_1, x_2, \dots, x_n)^T \in M$, where $M \subseteq \mathbb{R}^n$ is the state space, and T denotes the transpose operation. The state variable is a point in this n-dimensional state space. In a continuous-time dynamical system, the state evolves according to the equation:

$$\dot{x}(t) = f(x(t)) \quad (2.1)$$

where $f : M \rightarrow M$. Systems obeying Eq. 2.1 are deterministic: there is no randomness, no stochasticity, no noise. This means that, starting from one single state at time t , we can in principle describe the whole past and future evolution of the system. Furthermore, there is a lack of an explicit time dependence in f - i.e., $\partial f_i / \partial t = 0$ for $i = 1, \dots, n$. In this case, the dynamical system is said to be autonomous.

To obtain solutions to system 2.1 we need to provide one state, which we typically call an initial condition $x_0 = x(0) \in \mathbb{R}^n$. The combination of $\dot{x} = f(x)$ with $x(0) = x_0$ defines an initial value problem. A fundamental theorem makes our lives studying this problem much easier. This is the theorem of existence and uniqueness of solutions. For $x \in \mathbb{R}^n$ and $f : \mathbb{R}^n \rightarrow \mathbb{R}^n$, it requires that f is continuous and that all of its partial derivatives $\frac{\partial f_i}{\partial x_j}$, for $i, j = 1 \dots n$ are continuous in some open connected set $D \subset \mathbb{R}^n$. This basically means that it requires our function f to be sufficiently smooth. Then, for initial conditions $x_0 \in D$, the initial value problem has a solution $x(t)$ on some time interval $(-\tau, \tau)$ about $t = 0$, and the solution is unique! [59]

In state space, each solution describes a trajectory, a path, that goes through its initial condition x_0 . The uniqueness of solutions implies that, within this time interval $(-\tau, \tau)$, different trajectories do not intersect in state space. This is a crucial property underlying all systems we study.

A useful notation for the evolution of a continuous dynamical system is through the evolution operator $\Phi^t(x)$, which, informally defined, evolves the point x forward t time units. That is, $\Phi^t(x(0)) = x(t)$.

2.1.2 The fate of linear dynamical systems

Although trajectories do not cross, they can share the same fate, meaning they can converge to the region in state space. We can introduce this notion with a very simple mathematical example of a linear system. It has the form

$$\dot{x}(t) = Ax(t) \quad (2.2)$$

where A is a constant ($n \times n$) matrix.

If the eigenvalues $\lambda_i \in \mathbb{C}$ of A are all unique, its eigenvectors $v_i \in \mathbb{R}^n$ are linearly independent. Then, the general solution to this system can be written as Ref. [59]:

$$x(t) = \sum_{i=1}^n C_i e^{\lambda_i t} v_i. \quad (2.3)$$

Then, each initial condition determines the constant coefficients $C_i \in \mathbb{R}$. From Eq. 2.3 we can already notice that the origin of the system, $o = (0, \dots, 0)^T$, is a solution. In fact, it is an equilibrium: $\dot{x} = f(o) = 0$. A trajectory on the origin does not change over time.

As we see from Eq. 2.3, the behavior of trajectories depends on the eigenvalues λ_i of the matrix A . We can classify the equilibrium at the origin based on these eigenvalues, as shown in Fig. 2.1. If the real parts of all the eigenvalues are negative, then all trajectories in state space converge to the origin as $t \rightarrow \infty$. In this case, the origin is said to be a stable equilibrium (Figs. 2.1A-B). If at least one eigenvalue is negative, the trajectories diverge from the origin, which is then an unstable equilibrium (Figs. 2.1C-E). Stability here refers to the behavior of trajectories near the equilibrium. If it is stable, nearby trajectories converge to the equilibrium - or, equivalently, small perturbations that take a trajectory away from the equilibrium will eventually go back to the equilibrium. If it is unstable, then nearby trajectories diverge from it.

Stable equilibria are the only attracting solution, or attractor, of linear systems. In this case, although different trajectories cannot not intersect, they all converge to the origin as $t \rightarrow \infty$. In summary, the ultimate fate of linear systems is kind of boring: either trajectories end up at the origin or they diverge off to infinity. But the journey, the path that trajectories take before before the end, the *transient dynamics*, is more interesting. As shown in Fig. 2.1, this is dictated by the constellation of eigenvalues λ_i . For more details, the reader can refer to standard books on linear/nonlinear dynamics, such as Ref. [59].

2.1.3 The fate of nonlinear dynamical systems I: attractors

As just seen, stable equilibria are the only possible attractors in linear systems. Going beyond Eq. 2.2, nonlinear systems can have more interesting and complicated long-term dynamics (Fig. 2.2). Stable equilibria are still possible, as shown in Figs. 2.2A-B. The system here is a conductance-based neuronal model following equations [30]

$$\begin{aligned} \dot{x} &= (I - g_L(x_i - E_L) - g_{Na}m_\infty(x_i)(x_i - E_{Na}) - g_Ky_i(x_i - E_K))/C, \\ \dot{y} &= (n_\infty(x) - y_i)/\tau, \end{aligned} \quad (2.4)$$

with all parameters and functions defined in detail in Chapter ???. The input current I is chosen to be $I = 2.0$ so the system has excitable dynamics. Its state space is composed of a stable equilibrium, the only attractor, and two unstable equilibria, which create excitable dynamics. Excitability is a type of transient different than seen for linear systems. Some trajectories are forced to go on long excursions (excitations) before converging to the stable equilibrium. We study more about this again in Chapter ???.

Besides equilibria, nonlinear systems can also have periodic solutions. These orbits vary in time with a certain period T (Fig. 2.2C) and correspond to closed curves in state space (Fig. 2.2). In several cases these periodic solutions are isolated, in the sense that there are no other periodic orbits in some neighborhood around them. In that case, they are called limit cycles. The system used in this example is still the neuronal model of Eq. 2.4, but with a different parameter $I = 6$, which leads to the system now having a stable limit cycle. We see in this figure again an example of a long transient, with the trajectory initially going on a long excursion before converging to the limit cycle.

Not all curves in state space are closed, however. One can have quasiperiodic dynamics, in which trajectories never repeat exactly, although they might almost repeat. This is seen in Figs. 2.2E-F. Simulating the trajectory for longer times would fill up the figure more and more.

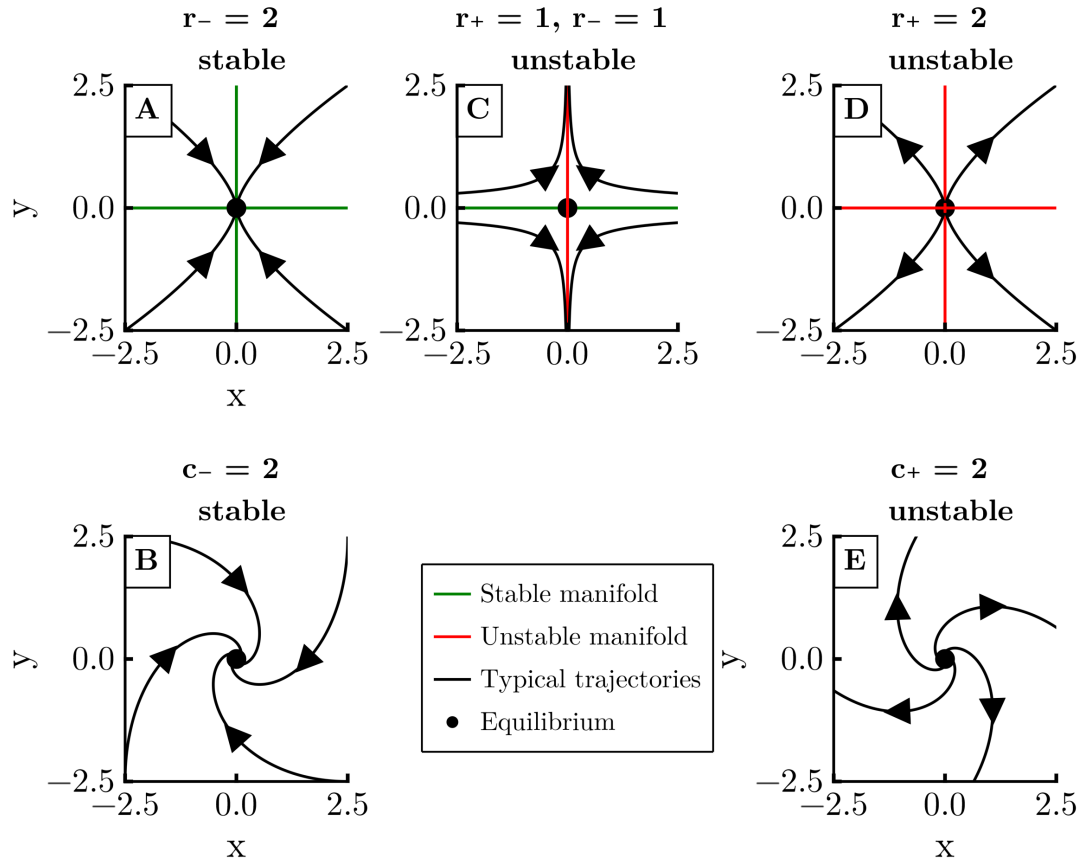


Figure 2.1: **Hyperbolic equilibria in 2D linear systems.** The title specifies the number of eigenvalues that are purely real negative r_- or positive r_+ , or that are complex with real part negative c_- or positive c_+ . The first row shows equilibria whose eigenvalues are purely real, while the second one shows equilibria with complex eigenvalues. In the first column, the equilibria are stable - they are the two possible attractors in linear systems. In the second column, we have a saddle-point for purely real eigenvalues. In the third column, the equilibria are completely unstable, known as repellers.

Further, note the varying amplitude of the time series. The system in this example is the forced Van der Pol oscillator,

$$\dot{x} = v \quad (2.5)$$

$$\dot{v} = \mu(1 - x^2)v - \alpha x + g \cos(\omega_f t), \quad (2.6)$$

with parameters $\mu = 0.1$, $\alpha = 1.0$, $g = 0.5$, $\omega_f = \sqrt{3}$ taken from Ref.[55].

Finally, one can also have chaotic attractors (Figs.2.2G-H). These solutions have a wild behavior that nearby trajectories tend to diverge at an exponential rate [6]. Despite this local divergence, however, the solutions remain bounded in space. In other words, systems with chaotic attractors are very sensitive to the initial conditions - small changes in initial conditions lead to trajectories that can look very different. The system used to generate is shown as the Lorenz system, with equations

$$\dot{x} = \sigma(y - x) \quad (2.7)$$

$$\dot{y} = x(\rho - z) - y \quad (2.8)$$

$$\dot{z} = x * y - \beta * z, \quad (2.9)$$

and $\sigma = 10$, $\rho = 28$, $\beta = 8/3$. This chaotic attractor in particular has a shape that resembles a butterfly, with trajectories spending some time on one wing before switching to the other wing [3].

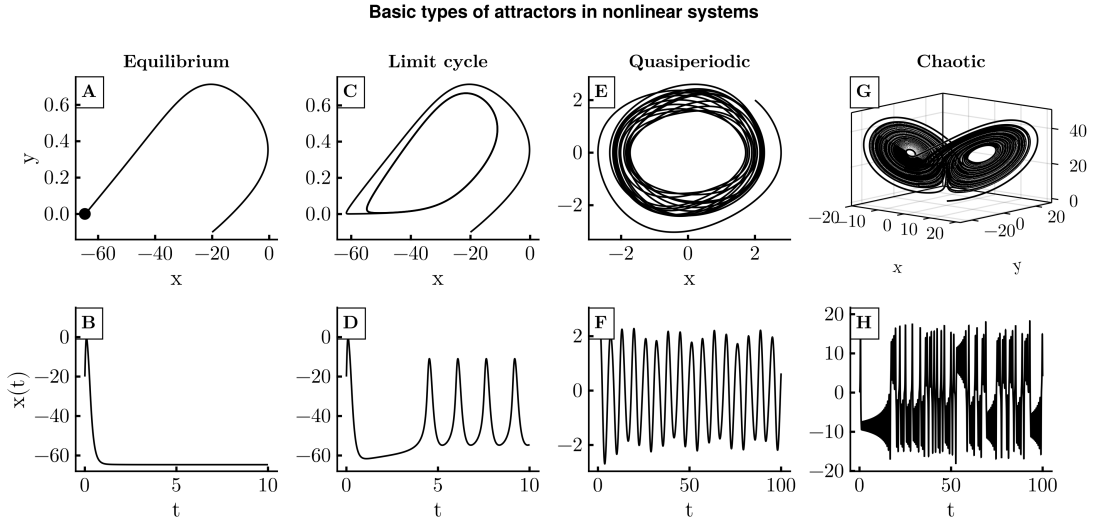


Figure 2.2: **Basic types of attractors in nonlinear dynamical systems.** Each column shows respectively the state space and a time-series of a typical trajectory converging to a type of attractor. The first column corresponds to the neuronal model of Eq.2.4 with $I = 2.0$, which has excitable dynamics, converging to a stable equilibrium. The second column shows again the neuronal system of Eq.2.4 but with $I = 6.0$, when the attractor is now a stable limit cycle. The third column shows the system defined in Eqs.2.6, with a quasiperiodic attractor. Finally, column four has an example of a chaotic trajectory on the Lorenz system (Eq. 2.9).

Given now these examples, let us now define the terms we have used a bit more properly.

2.1.4 Formalizing attractors and basins

We have just presented examples of attractors, sets of points in state space to which trajectories eventually converge, and their basins of attraction, the regions containing those converging trajectories. Since in this thesis we will deal a lot with these concepts, we provide now an attempt

at formalizing. The idea is to have the concepts clear in mind for later. In practice, we will only use the informal definition we just gave. In particular, the definition of attractor can vary considerably in the literature. Without attempting to claim any superiority, we attempt here to provide a definition that suits our studies.

First, we define an omega limit set $\omega(x)$ of a point $x_0 \in M$ as [41]:

$$\omega(x_0) = \{x : \forall T \forall \epsilon > 0 \text{ there exists } t > T \text{ such that } |f(x_0, t) - x| < \epsilon\}. \quad (2.10)$$

Consider a point $x \in \omega(x_0)$ in the ω limit set of x_0 . Then, by definition, a trajectory that passes through x_0 comes arbitrarily close to x infinitely often as t increases.

From this, we can define the *basin of attraction* of a set A as $\mathcal{B}(A) = \{x \in M : \omega(x) \subset A\}$. This only looks at the long-term behavior of trajectories; the transient dynamics could be anything, including the case that trajectories go very far from A , as long as they go back to it and stay there eventually.

Now to define an attractor, we first define a weaker (or, on the more optimistic side, a more general) version, called the *Milnor attractor*. It is a useful concept when dealing with metastability. A set A is a Milnor attractor if:

1. Its basin of attraction $\mathcal{B}(A)$ has strictly positive measure (i.e., if $m(\mathcal{B}(A)) > 0$), where $m(S)$ denotes a measure equivalent to the Lebesgue measure of set S [41]. This condition says that there is some probability that a randomly chosen point will be attracted to A [41].
2. For any closed proper subset $A' \subset A$, the set difference $\mathcal{B}(A) \setminus \mathcal{B}(A')$ also has strictly positive measure. This ensures that every part of A plays an essential role - one cannot decompose A into an attracting part and another part that does not attract [41, 62]. A closed set here means that it contains all its limit points. And proper means its non-empty.

Furthermore, the Milnor attractor does not have to attract all the points in its neighborhood, and there can also be orbits that transiently go very far from the attractor, even if initially close, before eventually getting close to it. Further, it can in principle be composed into the union of two smaller Milnor attractors. To avoid these cases, we call a set A an *attractor* if

1. A is a Milnor attractor.
2. A contains an orbit that is dense in A . Basically, this means that there is an orbit in A that passes arbitrarily close to every point in A . This condition ensures that the attractor is not the union of two smaller attracting sets [62].
3. There are arbitrarily small neighborhoods U of A such that $\forall x \in U$ one has $\Phi^t(x) \subset U \forall t > 0$ and such that $\forall y \in U$ one has $\omega(y) \subset \omega(x)$. That is, there are arbitrarily small neighborhoods around the attractor in which points inside stay inside and converge to A . This criterion is given in Ref. [6].

2.1.5 Invariant manifolds: structures that organize state space

In Sec. 2.1.2 we only considered the case when all the eigenvalues of the matrix A in the linear system $\dot{x} = Ax$ were positive. If one eigenvalue λ_k is positive, then trajectories will diverge to infinity following the corresponding eigenvector v_k . When some eigenvalues are positive, and some are negative, the origin is a saddle-point. If all eigenvalues are positive, it is called a repeller. Figure 2.1 shows examples of equilibria in 2D linear systems. Note that typical trajectories approach the saddle-point along the y -axis and then diverge along the x -axis. That is, for $t \rightarrow -\infty$, trajectories converge to the y -axis and for $t \rightarrow \infty$ they converge to the x -axis. The y -axis is called the stable manifold $\mathbb{W}^s(o)$ of the origin o and the x -axis is the unstable manifold $\mathbb{W}^u(o)$ of the origin. We can define these manifolds

$$\mathbb{W}^s(o) = \{x \in M : \Phi^t(x) \rightarrow o \text{ as } t \rightarrow \infty\}, \quad \mathbb{W}^u(o) = \{x \in M : \Phi^t(x) \rightarrow o \text{ as } t \rightarrow -\infty\}. \quad (2.11)$$

Let us separate the eigenvectors v_i into two parts: the ones with negative eigenvalues $v_1^-, \dots, v_{n_s}^-$ and the ones with positive eigenvalues $v_1^+, \dots, v_{n_u}^+$. Then we can define the stable and unstable subspaces, respectively, as

$$\mathbb{E}^s = \text{span}(v_1^-, \dots, v_{n_s}^-) \quad \mathbb{E}^u = \text{span}(v_1^+, \dots, v_{n_u}^+) \quad (2.12)$$

For a linear system, the stable manifold of the origin coincides with the stable space \mathbb{E}^s and the unstable manifold coincides with the unstable space. In general, as in the example of the saddle-point, these manifolds act to organize the behavior of trajectories in state space.

These concepts can be extended for nonlinear systems. To do this, the first step is to think about the linearization of the nonlinear system. Suppose our nonlinear system of interest has an equilibrium $x^* \in M$. It turns out that the behavior sufficiently close to this equilibrium is linear, despite the system globally being nonlinear [32, 21]! To see this, we first move the origin of our system to x^* by defining a new variable $y(t) = x(t) - x^*$. Then,

$$\dot{y} = \dot{x} = f(y + x^*) \equiv g(y) \quad (2.13)$$

where we define a convenience function $g(y)$. Expanding $g(y)$ around $y = 0$ (i.e., around the equilibrium $x(t) = x^*$) gives us

$$\dot{y} = g(0) + J_g(0)y + \mathcal{O}(y^2), \quad (2.14)$$

where $J_g(y) = \frac{\partial g_i(y)}{\partial y_j}$ is the Jacobian of g . It is related to the Jacobian of f by $J_g(y) = J_f(x)$, so $J_g(y=0) = J_f(x=x^*)$. Since $g(0) = f(x^*) = 0$, then if we are sufficiently close to the origin we can also ignore the terms $\mathcal{O}(y^2)$ and therefore we get

$$\dot{y} = J_g(0)y. \quad (2.15)$$

That is, the behavior of the nonlinear system sufficiently close to the equilibrium is linear, with the constant matrix function being the Jacobian evaluated at the equilibrium!

But the good news don't stop here! There is the Hartman-Grobman theorem, which basically shows that the state space near a hyperbolic equilibrium to the state space of the linearization. An equilibrium is hyperbolic if the eigenvalues of the Jacobian evaluated on it are all nonzero, i.e., if $\lambda_i \neq 0 \forall i = 1, \dots, n$. *Topologically equivalent* means that the linearized state space and the local state space near the equilibrium are distorted versions of each other. They can be bended and warped, but not ripped. In particular, closed orbits have to remain closed, and connections between saddle points have to remain [59]. Mathematically, topologically equivalent means there is a *homeomorphism* (continuous deformation with continuous inverse) from one state space into the other; trajectories can be mapped from one to the other, and the direction of time is the same [59].

Stating the theorem more formally, suppose a hyperbolic equilibrium $x^* \in M$ such that $f(x^*) = 0$ and such that all its eigenvalues are nonzero. Then, there is a neighborhood N of x^* and a homeomorphism $h : N \rightarrow M$ such that [3]

- $h(x^*) = 0$
- the flow $\dot{x} = f(x)$ in N is topologically conjugate to the flow of the linearization $\dot{y} = Ay$ by the continuous map $y = h(x)$. Topologically conjugate basically meaning a change of coordinates in a topological sense.

This guarantees that the stability of the equilibrium is the same in both cases, so we can use the linearization to gain important insights about the stability of equilibria in the nonlinear system!

What about the stable and unstable manifolds? In analogy to the linear case, we can define local stable and unstable sets near a neighborhood U of an equilibrium x^* for the nonlinear system [3]:

$$\mathbb{W}_{\text{loc}}^s(x^*) = \{x \in M : \Phi^t(x) \rightarrow o \text{ as } t \rightarrow +\infty \text{ and } \Phi^t(x) \in U \forall t \geq 0\}, \quad (2.16)$$

$$\mathbb{W}_{\text{loc}}^u(x^*) = \{x \in M : \Phi^t(x) \rightarrow o \text{ as } t \rightarrow -\infty \text{ and } \Phi^t(x) \in U \forall t \leq 0\}. \quad (2.17)$$

Herein comes the stable manifold theorem. It states that, for a hyperbolic equilibrium x^* :

- The local stable set $\mathbb{W}_{\text{loc}}^s(x^*)$ is a smooth manifold whose tangent space has the same dimension n_s as the stable space \mathbb{E}^s of the linearization of f at x^* . $\mathbb{W}_{\text{loc}}^s(x^*)$ is also tangent to \mathbb{E}^s at x^* .
- The local unstable set $\mathbb{W}_{\text{loc}}^u(x^*)$ is a smooth manifold whose tangent space has the same dimension n_u as the unstable space \mathbb{E}^u of the linearization of f at x^* . $\mathbb{W}_{\text{loc}}^u(x^*)$ is also tangent to \mathbb{E}^u at x^* .

The homeomorphism guaranteed by the Hartman-Grobman theorem maps $\mathbb{W}_{\text{loc}}^s(x^*)$ into \mathbb{E}^s and $\mathbb{W}_{\text{loc}}^u(x^*)$ into \mathbb{E}^u one-to-one, as shown in Fig. XX. Further, the stable manifold theorem guarantees that \mathbb{E}^s and \mathbb{E}^u actually approximate the local manifolds $\mathbb{W}_{\text{loc}}^s(x^*)$ and $\mathbb{W}_{\text{loc}}^u(x^*)$, respectively [3]. As a consequence, we get the behavior illustrated in Fig. 2.3

The manifolds we just looked at are defined for a local neighborhood U around the equilibrium. We can extend them towards the whole of state space by defining global manifolds as:

$$\mathbb{W}^s(x^*) = \bigcup_{t \leq 0} \Phi^t(\mathbb{W}_{\text{loc}}^s(x^*)) \quad (2.18)$$

$$\mathbb{W}^u(x^*) = \bigcup_{t \geq 0} \Phi^t(\mathbb{W}_{\text{loc}}^u(x^*)) \quad (2.19)$$

That is, the global stable manifold is obtained by integrating the local stable manifold backwards, looking at where the trajectories on it came from. For the unstable manifold, we integrate the local unstable manifold forwards, to see where it goes to.

An important fact about the local and global manifolds that follows from their definitions is that they are invariant: trajectories starting on these manifolds stay on them forever [3]. Furthermore, the uniqueness of solutions prohibits certain crossings of manifolds: stable manifolds of two distinct equilibria cannot cross, unstable manifolds of two distinct equilibria also cannot, and the same manifold cannot cross itself - otherwise, where the crossing points would have to obey two distinct paths! Meanwhile, stable and unstable manifolds, either of the same equilibrium or of two different equilibria can cross.

As mentioned before, these manifolds usually play a big role in organizing state space. As we will see in Chapter ??, they can organize the transient dynamics of systems. There, we study a dynamical system wherein certain trajectories are forced to go on long excursions before converging to the stable equilibrium, the only attractor in state space (see Figs.2.2A-B). As explained there, this long excursion is generated by the arrangement of the invariant manifolds of the saddle-point that exists in state space. The invariant manifolds can also organize the long-term behavior of systems: the next section briefly shows how stable manifolds of unstable equilibria can act as the boundary separating two basins of attraction.

2.1.6 The fate of nonlinear dynamical systems II: multistability and basins of attraction

In Sec. 2.1.3 we saw that the ultimate fate of nonlinear systems, their attractors, can be much more complicated than that of linear ones. Not only are the attractors themselves complicated, but they can also coexist in state space. If there are two coexisting attractors, this means that the state space will be separated into three regions: the basin of attraction of attractor one, the basin of attractor two, and the boundary between them. Usually, the basin boundary is formed by stable manifolds of saddle-type objects: saddle-points, saddle-limit-cycles, and even chaotic saddles! [47]. Figure 2.4 illustrates this for a relatively simple system with two stable equilibria, where the basin boundary is the stable manifold of the saddle-point in the middle. This system is known as the Duffing oscillator:

$$\dot{x} = v \quad (2.20)$$

$$\dot{v} = -(-kx + cv + lx^3)/m, \quad (2.21)$$

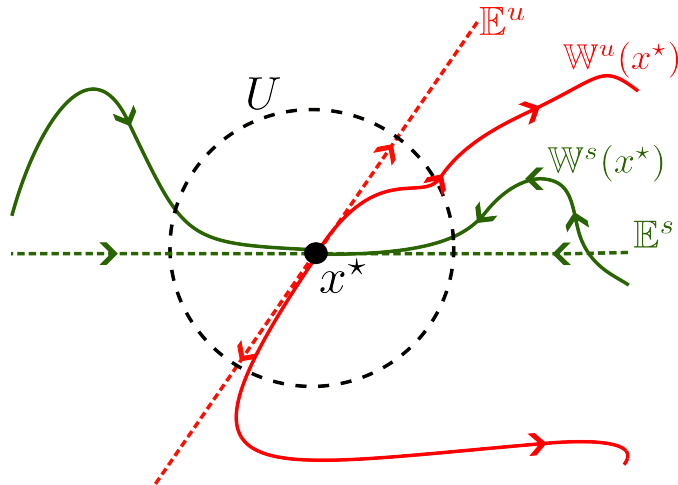


Figure 2.3: **Invariant manifolds of saddle point x^* .** The local stable $W_{\text{loc}}^s(x^*)$ and unstable $W_{\text{loc}}^u(x^*)$ manifolds of the saddle point x^* respectively can be associated with the stable E^s and unstable E^u subspaces and become tangent to them near the saddle. This follows from the Hartman-Grobman and the stable manifold theorems. The global stable $W^s(x^*)$ and unstable $W^u(x^*)$ manifolds extend the definition of the local manifolds beyond the neighborhood U . Figure is inspired by Fig. 6.2.4 from Ref. [3].

with $k = 1$, $c = 0.5$, $l = 1$, $m = 1$. This system represents a ball of mass m rolling downhill at position x and velocity v on a quartic potential landscape of the form $U(x) = -lx^4/4 - kx^2/2$ with a friction term $-cv$. Following the definition of global manifolds in Eq. 2.19, these global manifolds are essentially obtained by integrating trajectories starting on the local manifolds of the saddle-point.

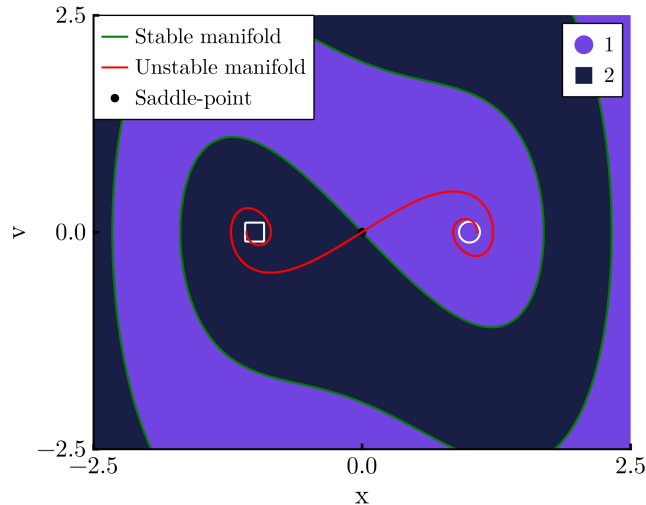


Figure 2.4: **Bistability in Duffing model.** Two stable equilibria (white square and circle) are shown with their respective basins of attraction in two shades of purple. The global stable and unstable manifolds of the saddle-point (black point) in the middle are also shown as green and red lines respectively. The global stable manifold of the saddle coincides with the boundary between the basins.

In this thesis we study two examples of multistability occurring in networked systems. In Chapter ?? we study networks of Kuramuro units, and see there the coexistence of multiple

attractors depending on how strongly the units are interacting. We also see how this multistability impacts the sensitivity of the system to small changes in parameters of the units. Later, in Chapter ?? we study how multistability arises when two excitable neurons are coupled together diffusively. Both studies require that we find the attractors in the systems. This is what we deal with in the next section.

2.1.7 How to find attractors

Finding all the attractors of a given dynamical system is not necessarily a trivial task. For equilibria, one can find all the roots of the system function, i.e., $f(x^*) = 0$ and then check their stability through the eigenvalues of the Jacobian evaluated on them. However, problem becomes more complicated for other types of attractors. To start off, simply proving that a set is an attractor, following the criteria given in Sec. 2.1.4, is usually not possible. Instead, in practice we use the looser definition of an attractor simply as the long-term dynamics of trajectories. Numerically, this means a brute-force approach of simulating several trajectories in state space for long integration times and seeing where they converge.

This comes with two problems. First, it does not rule out the possibility that a certain set is just a very long transient. To remedy this, we usually integrate trajectories on the set for very long and check if there is any escape. Second, some attractors might have very small basins of attraction, such that randomly chosen initial conditions are unlikely to end on them, so it is unlikely that we find those attractors. So far, however, this brute force approach is the best we have for general systems []. Within this approach, there are two main methods in the literature for finding attractors. They differ in how they check convergence to attractors.

The first approach was proposed in Ref. [43] and implemented with improvements in Ref. [12]. The idea is that a typical trajectory, initialized in a certain box in state space, will evolve, visiting other boxes, until it converges to the attractor. It will then stay on the attractor, repeatedly visiting the same state space boxes. Using this idea, the algorithm discretizes the state space into boxes, integrates trajectories, and looks for recurrences. Then, basically, when boxes are visited repeatedly a certain prescribed amount of times, then it considers that these boxes constitute the attractor. It is also smart in that it keeps track of the state of each box. So it knows that the boxes visited by the trajectory before converging to the attractor - the transient section of the trajectory - belongs to the basin of attraction of that attractor. This algorithm works really well for periodic, quasiperiodic, and chaotic attractors in low-dimensional systems. For chaotic attractors in high-dimensional systems it does not work well, because the time that trajectories take to recur on a chaotic attractor becomes too long to simulate numerically.

An alternative approach does not rely on discretizing state space, and is designed to work well for high-dimensional systems. In this case, one spreads a number N of initial conditions in state space and integrates them to obtain N trajectories. Each trajectory $x(t)$ is then converted to a vector of features $\mathcal{F} \in \mathbb{R}^n$ of n numbers that all collectively describe the trajectory. This is done by the featurizing function $\phi : M \times \mathbb{R} \rightarrow \mathbb{R}^n$, such that $\mathcal{F} = \phi(x(t), t)$. Each attractor should correspond to a unique \mathcal{F} . Then, the N vectors of features are grouped together via any of several possible grouping or clustering algorithms, and each grouping corresponds to one attractor. This approach can work very well, but it relies on pre-existing knowledge about the system to find a suitable featurizer function ϕ . To be confident about the results, one also has to verify that the total integration time is long enough, and that the transients of all trajectories were removed. This relies on experimentation. This method has been proposed in Ref. [20] and soon thereafter also in Ref. [58]. Together with colleagues, I implemented efficient and open-source code for this method with improvements in the Attractors.jl package Ref. [11].

Both methods can be applied across a parameter range and used in a continuation fashion, as illustrated in Fig. 2.1.7A. For the first parameter, the attractors of the system are found using any of the two methods just described. Then, points on these attractors are used as additional initial conditions for the next parameter value. The originally prescribed initial conditions, together with the original ones, are then used to find attractors in the subsequent parameter value. This process of seeding initial conditions from the previously found attractors is repeated for the whole parameter range. Then, one has all the attractors for each parameter value, and the remaining

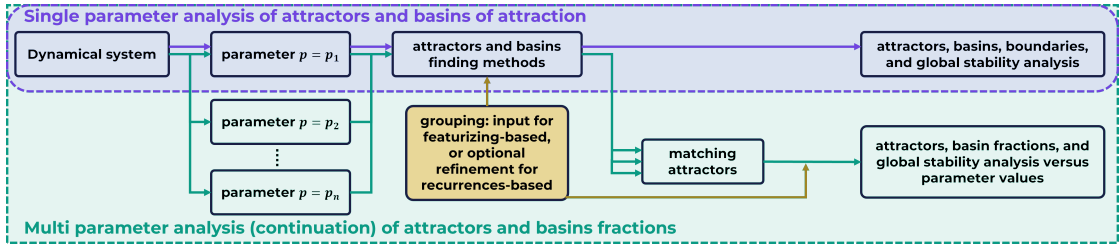


Figure 2.5: **Schematic illustration of the continuation method used to find and match attractors across a parameter range.** The first row illustrates the single-parameter attractor finding algorithms. The second row illustrates how they can be combined across parameters to perform a continuation analysis. Figure taken from Ref. [11].

problem is to link attractors from one parameter to the next. This matching of attractors is done by computing the distance between attractors at one parameter to attractors at the previous parameter, and matching the attractors by the shortest distance. The distance metric can be chosen by the user, including Euclidean distance between the centroids of the attractors, or a Hausdorff distance, or distance between the features of the attractors. I have also collaborated in the implementation of this method in efficient and open-source code, described in the publication in Ref. [11].

2.2 Bifurcations

What happens to the attractors - and, in general, to the state space structures - of a dynamical system when we vary its parameters? In terms of the qualitative properties, there are two possibilities: either they stay similar or they change drastically. We can be a bit more rigorous. Two systems are qualitatively similar if they are topologically equivalent. The notion of topological equivalence was already mentioned in Sec. 2.1.5. As a reminder, two systems are topologically equivalent if the state space of one can be obtained by a continuous transformation of the other [37]. Mathematically, this means that they are topologically equivalent if there is a homeomorphism $h : M \rightarrow M$ mapping orbits of the first system onto orbits of the second, preserving the direction of time.

As the parameters of a system are varied, we obtain different dynamical systems that are usually topologically equivalent. The attractors, for instance, may move, but they retain their stability. At some point, however, there may be a drastic change, and the new system may no longer be equivalent. The attractor may have disappeared, or lost its stability. Or a new attractor may have emerged. These drastic qualitative changes in the behavior of a dynamical system are called bifurcations. A bit more rigorously, a bifurcation is a change in the topological type of a system as its parameters pass through a critical (bifurcation) value [37]. There are many different types of bifurcations, and one can literally write a whole book about this [37]. For this thesis we focus briefly on just a few bifurcations that will be relevant for later. For simplicity, we focus also on the simplest version of these bifurcations.

2.2.1 Saddle-node bifurcation of equilibria

In a saddle-node bifurcation of equilibria we see the emergence, or destruction, of a stable (node) and an unstable (saddle) equilibrium. Starting from the side of the bifurcation in which the equilibria exist and approaching the bifurcation parameter, we see the equilibria approaching each other, coalescing at the critical parameter, and annihilating each other thereafter. The simplest form of this bifurcation occurs in one dimension in the system

$$\dot{x} = f(x) = \alpha + x^2, \quad (2.22)$$

with the critical value of the bifurcation being $\alpha = 0$. As shown in Figs. 2.6, for $\alpha < 0$ we see that the parabola $f(x)$ has two roots, so the system has two equilibria, in positions $x^* = \pm\sqrt{-\alpha}$. From the figure directly we can already see that the equilibrium on the left is stable and the equilibrium on right is unstable. We can confirm this with a linearization analysis - the Jacobian here is simply $df/dx = 2x$, so the eigenvalue of the left and right equilibrium are $-2\sqrt{-\alpha}$ and $+2\sqrt{-\alpha}$. As α increases towards 0 the parabola moves up, the equilibria approach each other, their eigenvalues approach zero, and at $\alpha = 0$ they all coalesce into one single equilibrium. At this point, the eigenvalue of the system is zero: this equilibrium is non-hyperbolic! For $\alpha > 0$ there are no more equilibria. Equation 2.22 is called the normal form of the saddle-node bifurcation, because any generic system obeying some conditions will be topologically equivalent to it locally, near the equilibrium. For a system $\dot{x} = f(x, p)$, with $x \in \mathbb{R}$ and $p \in \mathbb{R}$, $\partial f(0, 0)/\partial x = 0$, an equilibrium $x = 0$ at the critical parameter $\alpha = 0$, the conditions are [37]:

$$\frac{\partial^2 f(0, 0)}{\partial x^2} \neq 0 \quad (2.23)$$

$$\frac{\partial f(0, 0)}{\partial \alpha} \neq 0. \quad (2.24)$$

They guarantee that the system $\dot{x} = f(x, p)$ can be transformed into Eq. 2.22 or into $\dot{x} = \alpha - x^2$, which just inverts the direction of α .

After the two equilibria are destroyed, the system does not have an Just after the bifurcation, the region previously occupied by the two equilibria is still quite slow. Note how \dot{x} is very close to zero near $x = 0$ in Fig. 2.6. This region of slow flow is called the ghost of the saddle-node [59]. In a way, it retains properties of the two equilibria - particular, trajectories still flow towards the ghost from the side previously occupied by the stable equilibrium, remain in its neighborhood for a while, but then eventually depart through the side previously occupied by the unstable equilibrium [34]. The ghost is not an invariant set, but is an example of a metastable regime, which we study in greater depth in Chapter ??.

Saddle-node bifurcations can also occur analogously for periodic orbits [37] - a stable limit cycle then collides with an unstable limit cycle, and leave behind a ghost of a limit cycle!

2.2.2 Hopf bifurcation

Keeping with the spirit of describing the simplest cases, let us now imagine a system written in polar coordinates (ρ, θ) :

$$\dot{\rho} = f_\rho = \rho(\alpha - \rho^2) \quad (2.25)$$

$$\dot{\phi} = f_\phi = 1. \quad (2.26)$$

Because the two equations are decoupled, we can analyse the ρ equation separately first. First, note that its Jacobian $\partial f_\rho / \partial \rho = \alpha - 3\rho^2$. For all values of α , f_ρ has an equilibrium at $\rho = 0$ - with eigenvalue $\lambda = \alpha$. This is linearly stable for $\alpha < 0$ and linearly stable for $\alpha > 0$. At $\alpha = 0$ it is non-hyperbolic! What happens then? The first equation has another root for $\alpha > 0$ at $\rho = \sqrt{\alpha}$ - so the eigenvalue is $\lambda = -2\alpha$. This equilibrium is unstable for $\alpha < 0$ and stable for $\alpha > 0$. Notice the change of stability of the equilibria: when one is unstable, the other is stable, and vice versa. Considered for f_ρ alone, this is an example of a Pitchfork bifurcation [37]. Considering the full system, with the rotation induced by $\dot{\phi} = 1$, the equilibrium at the origin remains an equilibrium, but the equilibrium at $\sqrt{\alpha}$ becomes a limit cycle with amplitude $\sqrt{\alpha}$. Putting everything together, we have the behavior in Fig. 2.6G-H. A stable limit cycle becomes unstable at $\alpha = 0$ and from it a stable limit cycle emerges. This is called a supercritical Hopf bifurcation [37]. If we write this system in Cartesian coordinates and compute the eigenvalues of the Jacobian at the origin, we see they are $\lambda_{1,2} = \alpha \pm i$. This gives us another general property of this bifurcation: at the critical point, the eigenvalues at the origin cross the imaginary axis.

Now consider the system

$$\dot{\rho} = f_\rho = \rho(\alpha + \rho^2) \quad (2.27)$$

$$\dot{\phi} = f_\phi = 1. \quad (2.28)$$

Now the Jacobian is $\partial f_\rho / \partial \rho = \alpha + 3\rho^2$. There is still an equilibrium at the origin, in which the eigenvalue is still α - its stability is the same as before. However, the other equilibrium, now $\sqrt{-\alpha}$ has the associated eigenvalue as -2α . It therefore exists for $\alpha < 0$ when it is unstable. This thus corresponds to an unstable limit cycle, which coexists with a stable equilibrium for $\alpha < 0$. For $\alpha > 0$, the limit cycle disappears and the system is left with only an unstable equilibrium. This is called a subcritical Hopf bifurcation [37]. The eigenvalues of the Cartesian Jacobian at the origin behave in the same way as for the supercritical Hopf.

2.2.3 Homoclinic bifurcation

Both the saddle-node and the Hopf bifurcations happen in the neighborhood of equilibria - for this reason, they are called local bifurcations. Now we move to a bifurcation in which this is no longer the case - the state space beyond only the equilibrium is affected, and it is thus called a global bifurcation [37]. The formal description of this bifurcation is consequently more involved, and goes beyond the scope of this thesis. For here it is enough to describe the bifurcation more qualitatively.

In the homoclinic bifurcation we study here, occurring on the plane, we have the emergence of a stable or an unstable limit cycle. Before the bifurcation, there is only a saddle point. At the bifurcation, the unstable manifold of the saddle becomes tangential to its own stable manifold - this constitutes a homoclinic orbit. After the bifurcation, the homoclinic orbit becomes a limit cycle whose stability depends on the eigenvalues of the saddle. Defining the saddle quantity $\sigma = \lambda_1 + \lambda_2$, it can be shown [37] that the limit cycle is stable for $\sigma < 0$ and unstable if $\sigma > 0$.

Varying the bifurcation parameter α close to the homoclinic orbit, the limit cycle approaches more and more the saddle point, and touches it at $\alpha = \alpha_c$. The region of the limit cycle close to the saddle-point has a very slow dynamics, such that the period of the limit cycle diverges to infinity as the critical point is approached. In higher dimensional systems, different types of homoclinic bifurcations are possible, with potentially much more complicated dynamics. The homoclinic bifurcations we deal with in this thesis are always related to simple saddle points, and so are analogous to the planar case shown now.

An example of a planar system with this bifurcation is due to Sandstede [54]

$$\dot{x} = -x + 2y + x^2 \quad (2.29)$$

$$\dot{y} = (2 - \alpha)x - y - 3x^2 + (3/2)xy. \quad (2.30)$$

The origin is a saddle which, at $\alpha = 0$, has eigenvalues $\lambda_1 = 1$ and $\lambda_2 = -3$ - its saddle quantity is therefore $\sigma = 2 < 0$, so the limit cycle that emerges here is stable [37].

2.3 Basics of network theory

An incredibly powerful abstraction about real-world systems can be achieved through the concept of networks, here used as synonyms for graphs, which are composed of nodes that are connected by edges. Networks can represent friendships - with people being the nodes and their friendships being the edges -, brain circuits - neurons are nodes, synapses are edges [9] -, ecological systems - for instance, ecological regions are nodes, and migrations between them are edges [38]. In this thesis we make use of this abstraction and consider that the nodes are dynamical systems $\dot{x}_i = f(x_i)$, $x_i \in \mathbb{R}^n$ on their own, with certain interactions between them. Together, the whole networked system is a dynamical system of the form:

$$\dot{x}_i = f(x_i) + \sum_{j=1}^N A_{ij}g(x_j, x_i), \quad i = 1, \dots, N \quad (2.31)$$

with N units, whose interactions are described by the function g . The adjacency matrix A_{ij} describes the strength of interactions between the units. Typically it is a binary matrix, such that $A_{ij} = 1$ if unit i receives a connection from unit j and $A_{ij} = 0$ otherwise. It can also be

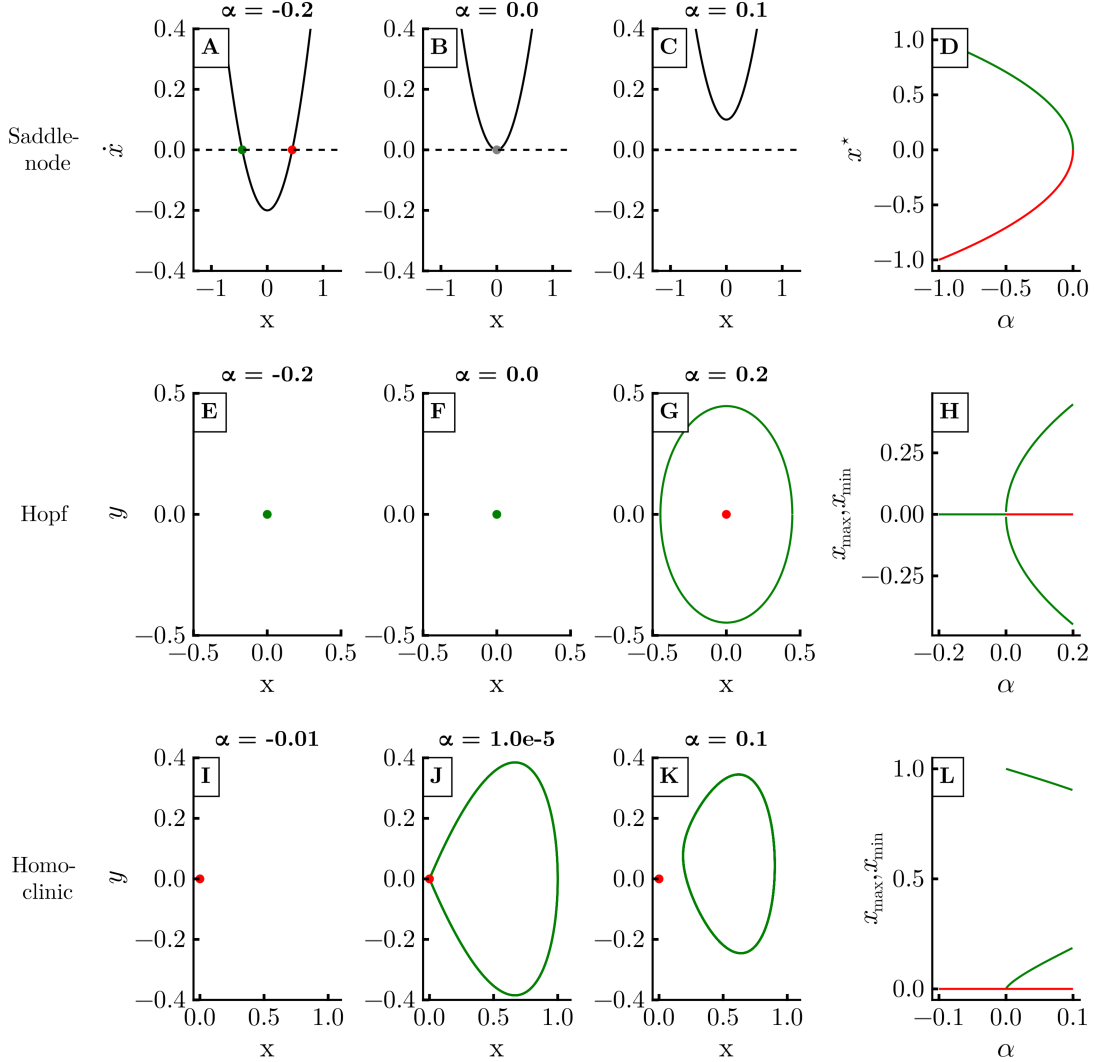


Figure 2.6: **Some important bifurcations.** The saddle-node bifurcation is shown for the normal form $\dot{x} = x^2 + \alpha$ in panels A-D. A stable and an unstable equilibria, represented respectively by green and red circles (panel A), come together as the bifurcation parameter α is changed. Eventually they coalesce (panel B) and are subsequently destroyed (panel C). The position of these equilibria as a function of α is shown in panel D. The supercritical Hopf bifurcation is shown for Eq. 2.25 in panels E-H. Before and at the bifurcation there is a stable equilibrium in state space (panels E and F respectively), which becomes unstable when a stable limit cycle emerges (panel G). Panel H shows this behavior as a function of α , taking the maximum and minimum values of x to represent the limit cycle. The homoclinic bifurcation to a saddle point is shown in panels I-L. Before the bifurcation there is a saddle point (panel I). At the bifurcation, an orbit homoclinic to this saddle point appears (represented approximately in panel J). After the bifurcation, a stable limit cycle emerges (panel K). This is also summarized in panel L.

weighted, in which case the entry $A_{ij} \in \mathbb{R}$ represents the strength of interactions. Usually for binary matrices, we rewrite Eq. 2.31 as

$$\dot{x}_i = f(x_i) + \sum_{j \in \Omega_i} g(x_j, x_i), \quad i = 1, \dots, N \quad (2.32)$$

where $\Omega_i = \{j \in [1, N] : A_{ij} = 1\}$ is called the neighborhood of unit i . The number of elements in Ω_i , i.e., the number of connections of unit i , is called the unit's degree.

The adjacency matrix A describes the topology of the network, meaning the architecture of the connections. There are many different types of topologies, which describe well different types of systems. One type of topology is the regular, also called k -nearest-neighbors topology. As the name suggests, one can think of all nodes arranged on a ring, with each node connected to the k nearest nodes on each side. Another type of topology is the random topology, in which connections are chosen at random between the nodes. One consider the regular and random topologies as two extremes, and interpolate between them in what is called the Watts-Strogatz algorithm [66]. In this case, one starts with a k -nearest neighbor ring of nodes. Then, choose connections with a probability p . For each chosen connection (i, j) , keep the source node i , randomly choose a new node j' in the network, and switch (i, j) to (i, j') . This effectively switches short-range connections (between nearest nodes) to long range connections (between nodes that are potentially far away). For this rewiring probability p at $p = 0$ one has the regular topology; for $p = 1$ one has the random topology.

Informally speaking, a regular network is considerably clustered, with its short-range structures. And the average distance (in terms of numbers of edges) in the network is considerably high. In a random network, clustering is very small, but the average distance is small. One can formalize these concepts and show how this transition occurs as p is changed [66]. Here, we mention that, when p is relatively small, only a few short-range connections are rewired as long-range. This does not change the clustering characteristics much, but considerably lowers the average distance between nodes - those few long-range connections act as efficient shortcuts between nodes. Networks in this regime are usually called small-world networks [66].

In Chap. ?? we also study distance-dependent networks. The adjacency matrix is then defined as

$$A_{ij} = \frac{1}{\eta(\alpha)(d_{ij})^\alpha}, \quad (2.33)$$

with $d_{ij} = \min(|i - j|, N - |i - j|)$ is the edge distance along the ring, and $\eta(\alpha) = \sum_{j=1}^{N'} \frac{2}{j^\alpha}$ is a normalization term. All units are thus connected, but the weight of the connections decays with the distance following the α parameter. This parameter can also be called the locality parameter, since $\alpha = 0$ leads to an all-to-all equally connected network and $\alpha \rightarrow \infty$ leads to a first-nearest-neighbor topology ($k = 1$). In between we get distance-dependent weights.

2.4 Basics of Kuramoto oscillators

2.4.1 Derivation of the model and transition to synchronization

The Kuramoto model, written in general as

$$\dot{\theta}_i = \omega_i + \epsilon \sum_{j=1}^N A_{ij} \sin(\theta_j - \theta_i) \quad (2.34)$$

serves as a paradigm for studies on synchronization phenomena [4]. Its usefulness comes it being simple enough to be mathematically tractable, sufficiently generic, and also complex enough to display interesting dynamics. To reach it, Kuramoto started from generic oscillators near supercritical Hopf bifurcations. Each unit i follows

$$\dot{Q}_i = (i\omega + \alpha)Q_i - \beta|Q_i|^2Q_i, \quad (2.35)$$

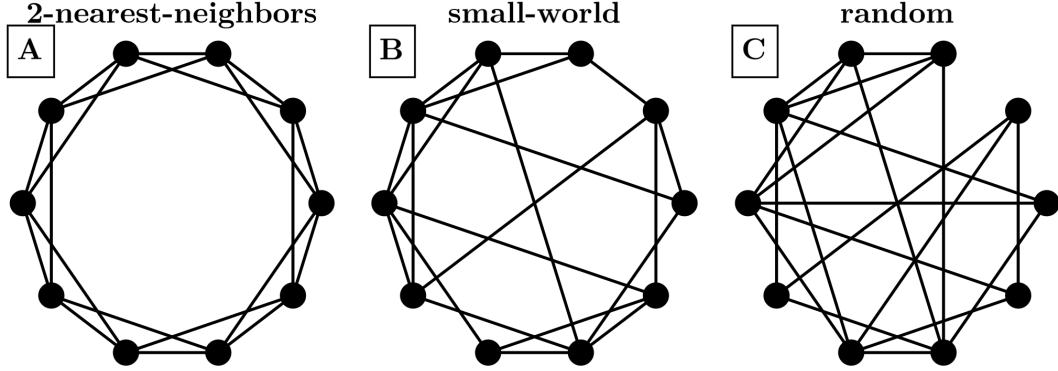


Figure 2.7: **Illustration of networks generated by the Watts-Strogatz procedure.** First, a k -nearest neighbor topology is created (Panel A). Then, some connections are randomly rewired, keeping the source node but changing the target node. With a few rewirings, this creates small-world networks (Panel B). With many rewirings, the network becomes randomly connected (Panel C).

where ω is the natural frequency of the oscillator, $\alpha > 0$ and $\beta > 0$ are parameters and $Q \in \mathbb{C}$. This is the normal form of the Hopf bifurcation we saw in Sec.2.2 but written in complex numbers. Kuramoto chose a simple and natural way to couple these oscillators: via a common coupling term, that is proportional to the value Q_i of each oscillator:

$$\dot{Q}_i = (i\omega + \alpha)Q_i - \beta|Q_i|^2Q_i + \frac{K}{N} \sum_{j=1}^N Q_j \quad (2.36)$$

which corresponds to an all-to-all topology, with K being the coupling strength. Here the natural frequencies are assumed to be drawn from a certain distribution $g(\omega)$, usually unimodal.

One can then rewrite (2.36) in polar coordinates by using $Q_i = e^{i\theta_i}\rho_i$. Substituting it one gets the equations

$$\dot{\rho}_i = (\alpha - \beta\rho_i^2) + \frac{K}{N} \sum_{j=1}^N \rho_j \cos(\theta_j - \theta_i) \quad (2.37)$$

$$\dot{\theta}_i = \omega_i + \frac{K}{N} \sum_{j=1}^N \frac{\rho_j}{\rho_i} \sin(\theta_j - \theta_i) \quad (2.38)$$

Kuramoto studied these equations in the limit of $\alpha \rightarrow \infty$ and $\beta \rightarrow \infty$ with α/β constant. Then, one gets that the radial variables ρ_i approach a stable fixed point in arbitrarily fast. The radial variable is therefore just a constant and one just needs to consider the phase variables:

$$\theta_i = \omega_i + \frac{K}{N} \sum_{j=1}^N \sin(\theta_j - \theta_i). \quad (2.39)$$

A very useful way to quantify the spread of the phases θ_i is through the complex order parameter:

$$Z = re^{i\psi} = \frac{1}{N} \sum_{j=1}^N e^{i\theta_j}, \quad (2.40)$$

which corresponds to the centroid of the phases and therefore characterizes well the collective behavior of the system. The radius r measures the phase synchronization of the system: r is close to 0 if the phases are uniformly spread or clustered in anti-phase clusters and r is close to 1 if the phases are aligned together. Here we should clarify that phase synchronization denotes the alignment of phases of oscillations - complete phase synchronization corresponds to $r = 1$, meaning that the phases are the same (up to a 2π offsets). On the other hand, frequency synchronization denotes the alignment of the frequencies of oscillations - complete frequency synchronization corresponds to $\dot{\theta}_i = \Omega$, $\forall i = 1, \dots, N$. Networks that are frequency synchronized are also said to be phase-locked - the phase differences are constant. But it does not imply phase synchronization, as the phase differences may be non-zero. Figures 2.8A-B exemplify the behavior of r for weak and strong phase synchronization.

The angle ψ corresponds to the average phase of the units. Using this order parameter, the Kuramoto model can be rewritten as

$$\dot{\theta}_i = \omega_i + Kr \sin(\phi - \theta_i), \quad i = 1, \dots, N. \quad (2.41)$$

This form highlights the mean-field character of the model [60]. The oscillators now interact through the mean-field quantities r and ψ . The phase θ_i is pulled towards the mean phase ψ . And the effective coupling strength becomes Kr , so it is modulated by the degree of phase synchronization r . This creates a positive feedback loop, wherein as the system phase synchronizes more, the coupling becomes stronger and so the system tends to phase synchronize even more. This is a very clear mechanism for spontaneous synchronization [60].

These equations always have a solution for $\theta_i = 0, \forall i$. What about others? Kuramoto considered these equations in the infinite size limit $N \rightarrow \infty$. By seeking steady-state solutions, with r constant noted that oscillators will distribute into two groups: (i) with $|\omega_i| < Kr$ which phase-lock together and (ii) with $|\omega_i| > Kr$ which keep rotating with nonuniform velocity $\dot{\theta}_i$. He then showed that a branch continuously bifurcates from $r = 0$ at $K = K_c$, a critical coupling strength, given by:

$$K_c = \frac{2}{\pi g(0)} \quad (2.42)$$

Near $K = K_c$, this branch has a square-root behavior: $r \propto \sqrt{K - K_c}$. In particular for ω_i following a Lorentzian distribution, one can show that [36, 60]

$$r = \sqrt{1 - \frac{K_c}{K}}, \quad (2.43)$$

as illustrated in Fig. 2.8C. One can verify this behavior numerically: Fig. 2.8D illustrates the results of simulations for a network of $N = 1000$ oscillators under a Gaussian distribution with zero mean and unitary standard deviation. The y -axis denotes the time-averaged behavior of $r(t)$, which oscillates in time.

Many open questions remain from the treatment just shown, such as the stability of these branches. There have been many extensions made to this model [1, 51]. In the context of multistability, some basic results come from studying an even simpler configuration, where the units are identical and coupled in a k -nearest-neighbor ring.

2.4.2 Multistability in homogeneous case: twisted states

In the case of homogeneous oscillators with $\omega_i = \omega$ coupled in a k -nearest-neighbor topology, the equations become

$$\dot{\theta}_i = \omega + \epsilon \sum_{j=i-k}^{j=i+k} \sin(\theta_j - \theta_i). \quad (2.44)$$

One can switch to a corotating frame with angular velocity ω to get rid of the ω term and appropriately rescale time to get rid of ϵ and simplify down to

$$\dot{\theta}_i = \sum_{j=i-k}^{j=i+k} \sin(\theta_j - \theta_i). \quad (2.45)$$

Note therefore that changing the coupling strength in this system only rescales time, and does not change the state space significantly! This can be written as a gradient system $\dot{\theta} = -\nabla U(\theta)$, where $U(\theta)$ is a scalar differentiable function of $\theta \in \mathbb{R}^n$ [67, 59]. As a consequence, the only attractors in this system are equilibria [67]. Therefore to find all the attractors in the system one can first find the equilibria and then determine their linear stability. By doing this this, one finds that the equilibria obey the relation:

$$\theta_i = \omega t + \frac{2\pi q}{N} i + C \quad (2.46)$$

where $C \in \mathbb{R}$ is a constant and $q \in \mathbb{Z}$ is the twisting number. If one looks at the phase difference between two adjancent units one sees that it is constant across the ring: $\theta_{i+1} - \theta_i = \frac{2\pi q}{N}$. In particular, the completely synchronized is included here in the $q = 0$ case. Some important stability results are:

- For small values of k many twisted states can be stable. As k is increased, these twisted states start to lose stability, with higher q values starting earlier. Eventually, the completely synchronized state ($q = 0$) becomes globally stable at $k > k_c \approx 0.34N$ [67].
- If we fix k and look at estimates of the size of the basins of all stable twisted states we find that they can be parametrized by a Gaussian curve [67, 70] (Fig. 2.8E).
- Estimates of the size of the basin of attraction for $q = 0$ increase monotonically with k (Fig. 2.8F): the completely synchronized state starts to dominate the state space for denser networks [67].
- The shape of the basins is still a topic under research, but they appear to form octopus-like structures. The twisted state itself (a point) is on the head of the octopus, which a small volume around it. The majority of the volume of the basin is concentrated on the tentacles, which are structures that spread around in state space [70].

Studies have also been made for other topologies. Some important results have accumulated to show that networks with homogeneous frequencies are guaranteed to globally synchronize if the nodes are sufficiently well connected (if the networks are sufficiently dense). Taking the least connected node, with degree k_{\min} , and comparing it with the maximum possible degree of the network, $N - 1$, one can define the network's connectivity μ as the ratio $\mu = k_{\min}/(N - 1)$. Then, in networks with $\mu > \mu_c$, the only attractor is the fully synchronized state. Estimates have that $\mu \in [0.6818, 0.7889]$ [61, 65].

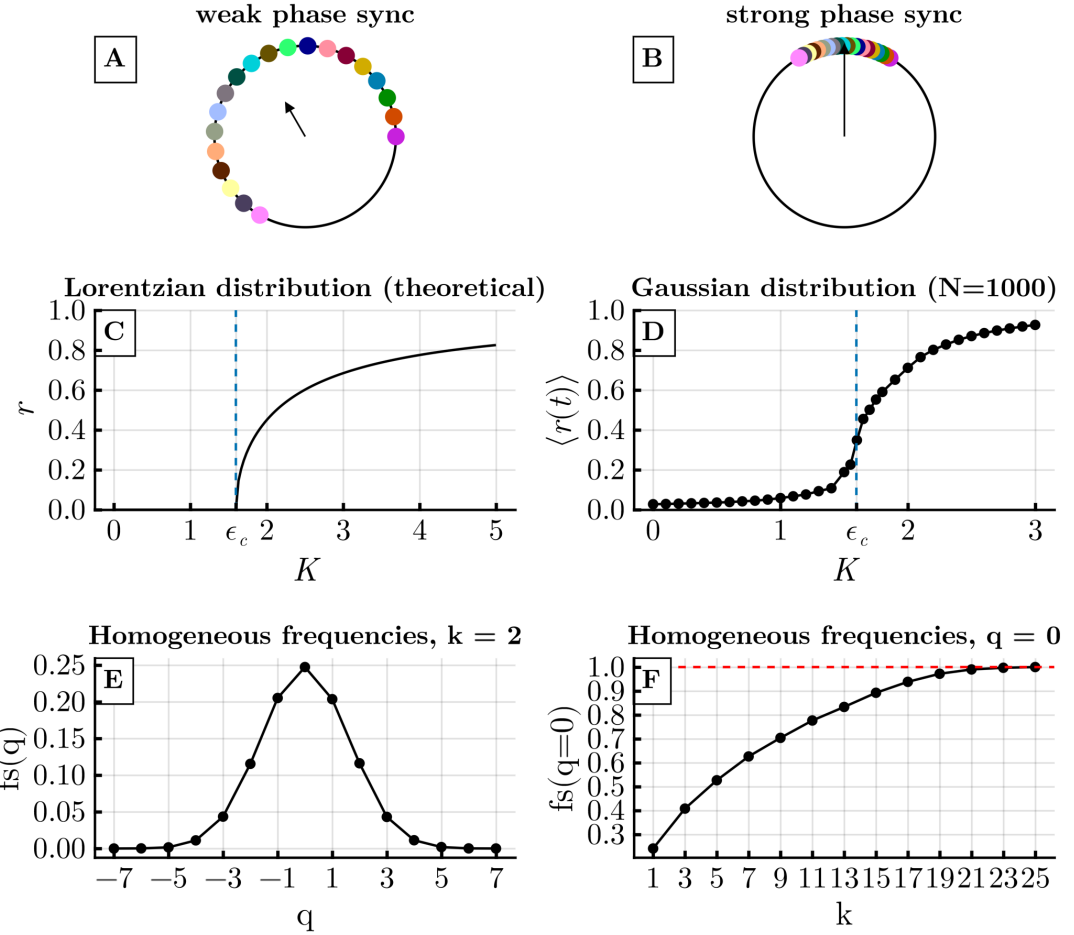


Figure 2.8: **Basics of Kuramoto oscillators.** Panels A and B respectively illustrate the concept of weak and strong phase synchronization (PS), captured by the complex order parameter Z (Eq. 2.40). The radius r denotes the degree of PS and the angle ψ denotes the centroid of the phases - respectively, they correspond to the magnitude and direction of the arrow in the figure. Panel C illustrates the behavior of the order parameter r as a function of coupling strength K (see Eq. 2.39) for a Lorentzian distribution of the frequencies (Eq. 2.43). The blue line denotes the critical coupling strength for the transition to synchronization. Panel D illustrates a similar behavior obtained from numerical simulations in a network of size $N = 1000$ under a Gaussian distribution of the natural frequencies. Only one attractor is ever observed in the simulations. Going now to homogeneous frequencies, panel E illustrates the fraction f_s of randomly chosen initial conditions that converge to each q twisted state, in a network with $k = 2$ nearest neighbors. Panel F looks at this fraction for the completely synchronized state ($q = 0$) only, under different values of k . Panels E and F replicate results from [67].

Chapter 3

Conclusions

Strogatz's idea: science is typically reductionist: break everything into small parts and understand them individually. The field of complex systems arises from the need to do go back, to do the inverse problem: construct the full system's behavior from its parts. As we have found out, interactions between even simple units can generate complicated behavior. A major challenge still today is to develop tools that allows us to characterize and figure out this behavior.

One such complicated behavior is the coexistence of multiple stable solutions to the same equation with the same parameters - multistability! How do these solutions come about, how are they organized in state space, how they are they separated in state space - these are all questions under active research.

Some of these stable solutions may correspond to synchronized regimes, which brings into light another important phenomenon: synchronization. Here again the field of complex systems has to contend with how individually distinct units can cooperate and start to operate in unison, in a beautiful example of an emerging phenomena. The study of synchronization - both frequency and phase synchronization - has important practical motivations, for instance in the study of power grids. Understanding the robustness of solutions in a complex network, in particular synchronized solutions has been an object of active research.

Combining these two research areas, Chapter ?? investigated the robustness of solutions in a complex network. For the study we chose the Kuramoto model, a paradigm for studies on synchronization phenomena and complex networks in general. The idea was to investigate how the network behaves, how the solutions change, when we change the parameter of a single unit in the network. We found that the dynamical malleability of the network depends on how strongly coupled the units are, and the topology of the connections. XX. We show that the mechanism driving this malleability are two: increased sample-to-sample fluctuations XX and multistability. We show that the number of attractors varies similarly to the dynamical malleability XX.

Contribution to understanding of both sync and multistability. Practical importance.

Open questions: malleability is very general; how is the multistability? Regardless, how does it emerge? How do the basins behave? One future work: burying under noise.

In a similar vein, we also investigated how multistability comes about when excitable neurons are coupled diffusively. powerful mechanism for generating multiple attractors. studied mainly coupling in x and y, but just in x is already enough.

based on the mechanism and preliminary results, we conjecture that topology plays a key role in dictating which attractors emerge. this is similar to kuramoto, and a more in depth comparison is definitely warranted.

didnt focus on sync, but we couldve: for $I=3.1$ XX. came into this problem when trying to figure out THE LOMBA. found out chaotic saddle was important but also slow region of LC generating multistability. Now we understand how slowness can help generate attractors in a simpler system, we can also go back to the original problem. generality of results is still a question.

XX

everything is a matter of time scales. if your observation time is long enough, compared to

the relaxation time to the attractors, then you see attractors. if it is not long enough, you dont have time to reach the attractors; you thus see transients. the former is a common case, but so is the latter, for instance in the brain where a lot of stuff is going on fast FAST I SAY. this is made more complicated due to the fact there are many mechanisms that can generate long transients. we saw one example of this in chap 3 with the excitability

to illustrate the importance of transients allow us to do a quick detour into TURING MACHINES. computation is done on the transient. plethora of observations in the literature. important works, lots of definitions, some proposals of mechanisms. lack of conceptual framework.

despite the initial motivation being to provide a nice definition, the work outgrew this and became a conceptual framework to think about metatsability, in what we believe is an important step toward a general understanding of transient dynamics.

computations, advantages

complex networks, topology, sync (harken back to daad proposal) toward complete understanding of the behavior of the system, on the attractors, and before trying to put all those pieces together

Acknowledgments

Write your acknowledgments here.

Bibliography

- [1] Juan A. Acebrón, L. L. Bonilla, Conrad J. Pérez Vicente, Félix Ritort, and Renato Spigler. The Kuramoto model: A simple paradigm for synchronization phenomena. *Reviews of Modern Physics*, 77(1):137–185, 2005.
- [2] Miri Adler, Avi Mayo, Xu Zhou, Ruth A. Franklin, Matthew L. Meizlish, Ruslan Medzhitov, Stefan M. Kallenberger, and Uri Alon. Principles of Cell Circuits for Tissue Repair and Fibrosis. *iScience*, 23(2):100841, 2020.
- [3] John H. Argyris, Gunter Faust, Maria Haase, and Rudolf Friedrich. *An Exploration of Dynamical Systems and Chaos*. Springer Berlin, Heidelberg, 2 edition, 2015.
- [4] Stefano Boccaletti, Alexander N. Pisarchik, Charo I. del Genio, and Andreas Amann. *Synchronization: From Coupled Systems to Complex Networks*. Cambridge University Press, 2018.
- [5] B. A. W. Brinkman, H. Yan, A. Maffei, I. M. Park, A. Fontanini, J. Wang, and G. La Camera. Metastable dynamics of neural circuits and networks. *Applied Physics Reviews*, 9(1):011313, 2022.
- [6] Henk Broer and Floris Takens. *Dynamical Systems and Chaos*. Applied Mathematical Sciences. 2011.
- [7] R. C. Budzinski, K. L. Rossi, B. R. R. Boaretto, T. L. Prado, and S. R. Lopes. Synchronization malleability in neural networks under a distance-dependent coupling. *Physical Review Research*, 2(4):043309, 2020.
- [8] Roberto C Budzinski, Alexandra N Busch, Samuel Mestern, Erwan Martin, Luisa H B Liboni, Federico W Pasini, Ján Mináć, Todd Coleman, Wataru Inoue, and Lyle E Muller. An exact mathematical description of computation with transient spatiotemporal dynamics in a complex-valued neural network. *arXiv*, 2023.
- [9] Ed Bullmore and Olaf Sporns. Complex brain networks: graph theoretical analysis of structural and functional systems. *Nature Reviews Neuroscience*, 10(3):186–198, 2009.
- [10] Giancarlo La Camera, Alfredo Fontanini, and Luca Mazzucato. Cortical computations via metastable activity. *Current Opinion in Neurobiology*, 58:37–45, 2019.
- [11] George Datseris, Kalel Luiz Rossi, and Alexandre Wagemakers. Framework for global stability analysis of dynamical systems. *Chaos: An Interdisciplinary Journal of Nonlinear Science*, 33(7):073151, 2023.
- [12] George Datseris and Alexandre Wagemakers. Effortless estimation of basins of attraction. *Chaos: An Interdisciplinary Journal of Nonlinear Science*, 32(2):023104, 2022.
- [13] Michael Dellnitz and Robert Preis. Symbolic and Numerical Scientific Computation, Second International Conference, SNSC 2001, Hagenberg, Austria, September 12–14, 2001. Revised Papers. *Lecture Notes in Computer Science*, pages 183–209, 2003.

- [14] Ulrike Feudel. Complex Dynamics In Multistable Systems. *International Journal of Bifurcation and Chaos*, 18(06):1607–1626, 2008.
- [15] Ulrike Feudel, Celso Grebogi, Leon Poon, and James A. Yorke. Dynamical properties of a simple mechanical system with a large number of coexisting periodic attractors. *Chaos, Solitons & Fractals*, 9(1-2):171–180, 1998.
- [16] Andrew Flynn and Andreas Amann. Exploring the origins of switching dynamics in a multifunctional reservoir computer. *Frontiers in Network Physiology*, 4:1451812, 2024.
- [17] Jennifer Foss, André Longtin, Boualem Mensour, and John Milton. Multistability and Delayed Recurrent Loops. *Physical Review Letters*, 76(4):708–711, 1996.
- [18] Pascal Fries. Rhythms for Cognition: Communication through Coherence. *Neuron*, 88(1):220–235, 2015.
- [19] Gary Froyland. Statistically optimal almost-invariant sets. *Physica D: Nonlinear Phenomena*, 200(3-4):205–219, 2005.
- [20] Maximilian Gelbrecht, Jürgen Kurths, and Frank Hellmann. Monte Carlo basin bifurcation analysis. *New Journal of Physics*, 22(3):033032, 2020.
- [21] Paul Glendinning. *Stability, Instability And Chaos: An Introduction To The Theory Of Nonlinear Differential Equations (cambridge Texts In Applied Mathematics)*. Cambridge Texts in Applied Mathematics. Cambridge University Press, Cambridge [England], 1 edition, 1994.
- [22] Mathieu Golos, Viktor Jirsa, and Emmanuel Daucé. Multistability in Large Scale Models of Brain Activity. *PLoS Comput Biol*, 11(12):1004644, 2015.
- [23] Peter beim Graben, Antonio Jimenez-Marin, Ibai Diez, Jesus M. Cortes, Mathieu Desroches, and Serafim Rodrigues. Metastable Resting State Brain Dynamics. *Frontiers in Computational Neuroscience*, 13:62, 2019.
- [24] Lukas Halekotte, Anna Vanselow, and Ulrike Feudel. Transient chaos enforces uncertainty in the British power grid. *Journal of Physics: Complexity*, 2(3):035015, 2021.
- [25] Frank Hellmann, Paul Schultz, Patrycja Jaros, Roman Levchenko, Tomasz Kapitaniak, Jürgen Kurths, and Yuri Maistrenko. Network-induced multistability through lossy coupling and exotic solitary states. *Nature Communications*, 11(1):592, 2020.
- [26] J L Hindmarsh and R M Rose. A model of neuronal bursting using three coupled first order differential equations. *Proceedings of the royal society of London B: biological sciences*, 221(1222):87–102, 1984.
- [27] Hyunsuk Hong, Hugues Chaté, Hyunggyu Park, and Lei Han Tang. Entrainment transition in populations of random frequency oscillators. *Physical Review Letters*, 99(18):1–4, 2007.
- [28] Hyunsuk Hong, Hyunggyu Park, and Lei Han Tang. Finite-size scaling of synchronized oscillation on complex networks. *Physical Review E*, 76(6):1–7, 2007.
- [29] Silvan Hürkey, Nelson Niemeyer, Jan-Hendrik Schleimer, Stefanie Ryglewski, Susanne Schreiber, and Carsten Duch. Gap junctions desynchronize a neural circuit to stabilize insect flight. *Nature*, 618(7963):118–125, 2023.
- [30] Eugene M Izhikevich. *Dynamical systems in neuroscience*. MIT press, 2007.
- [31] Lauren M. Jones, Alfredo Fontanini, Brian F. Sadacca, Paul Miller, and Donald B. Katz. Natural stimuli evoke dynamic sequences of states in sensory cortical ensembles. *Proceedings of the National Academy of Sciences*, 104(47):18772–18777, 2007.

- [32] Jorge V. José and Eugene J. Saletan. *Classical Dynamics: A Contemporary Approach*. Cambridge University Press, Cambridge, 1998.
- [33] Tahmineh Khazaei, Rory L. Williams, Said R. Bogatyrev, John C. Doyle, Christopher S. Henry, and Rustem F. Ismagilov. Metabolic multistability and hysteresis in a model aerobe-anaerobe microbiome community. *Science Advances*, 6(33):eaba0353, 2020.
- [34] D. Koch, A. Nandan, G. Ramesan, I. Tyukin, A. Gorban, and A. Koseska. Ghost Channels and Ghost Cycles Guiding Long Transients in Dynamical Systems. *Physical Review Letters*, 133(4):047202, 2024.
- [35] Daniel Koch, Akhilesh Nandan, Gayathri Ramesan, and Aneta Koseska. Biological computations: Limitations of attractor-based formalisms and the need for transients. *Biochemical and Biophysical Research Communications*, 720:150069, 2024.
- [36] Yoshiki Kuramoto. *Chemical Oscillations, Waves, and Turbulence*, volume 19 of *Springer Series in Synergetics*. Springer Berlin Heidelberg, Berlin, Heidelberg, 1984.
- [37] Yuri A. Kuznetsov. Elements of Applied Bifurcation Theory. *Applied Mathematical Sciences*, 2004.
- [38] Pietro Landi, Henintsoa O. Minoarivelo, Åke Brännström, Cang Hui, and Ulf Dieckmann. Complexity and stability of ecological networks: a review of the theory. *Population Ecology*, 60(4):319–345, 2018.
- [39] Everton S. Medeiros, Rene O. Medrano-T, Iberê L. Caldas, and Ulrike Feudel. Boundaries of synchronization in oscillator networks. *Physical Review E*, 98(3):030201, 2018.
- [40] Everton S. Medeiros, Rene O. Medrano-T, Iberê L. Caldas, Tamás Tél, and Ulrike Feudel. State-dependent vulnerability of synchronization. *Physical Review E*, 100(5):052201, 2019. Publisher: American Physical Society.
- [41] John Milnor. On the concept of attractor. *Communications in Mathematical Physics*, 99(2):177–195, 1985.
- [42] Akhilesh Nandan, Abhishek Das, Robert Lott, and Aneta Koseska. Cells use molecular working memory to navigate in changing chemoattractant fields. *eLife*, 11:e76825, 2022.
- [43] Helena E. Nusse, James A. Yorke, and Eric J. Kostelich. Dynamics: Numerical Explorations, Accompanying Computer Program Dynamics. *Applied Mathematical Sciences*, 1994.
- [44] Franziska Peter and Arkady Pikovsky. Transition to collective oscillations in finite Kuramoto ensembles. *Physical Review E*, 97(3):032310, 2018.
- [45] Arkady Pikovsky, Michael Rosenblum, and Jürgen Kurths. *Synchronization: A Universal Concept in Nonlinear Science*, volume 70. Cambridge University Press, 2001.
- [46] Alexander N. Pisarchik and Ulrike Feudel. Control of multistability. *Physics Reports*, 540(4):167–218, 2014.
- [47] Alexander N. Pisarchik and Alexander E. Hramov. Multistability in Physical and Living Systems, Characterization and Applications. *Springer Series in Synergetics*, 2022.
- [48] Max Potratzki, Timo Bröhl, Thorsten Rings, and Klaus Lehnertz. Synchronization dynamics of phase oscillators on power grid models. *Chaos: An Interdisciplinary Journal of Nonlinear Science*, 34(4):043131, 2024.
- [49] Erzsébet Ravasz Regan and William C. Aird. Dynamical Systems Approach to Endothelial Heterogeneity. *Circulation Research*, 111(1):110–130, 2012.
- [50] Alexander Robinson, Reinhard Calov, and Andrey Ganopolski. Multistability and critical thresholds of the Greenland ice sheet. *Nature Climate Change*, 2(6):429–432, 2012.

- [51] Francisco A. Rodrigues, Thomas K.D.M. Peron, Peng Ji, and Jürgen Kurths. The Kuramoto model in complex networks. *Physics Reports*, 610:1–98, 2016.
- [52] K. L. Rossi, R. C. Budzinski, B. R. R. Boaretto, T. L. Prado, U. Feudel, and S. R. Lopes. Phase-locking intermittency induced by dynamical heterogeneity in networks of thermosensitive neurons. *Chaos: An Interdisciplinary Journal of Nonlinear Science*, 31(8):083121, 2021.
- [53] Kalel L. Rossi, Roberto C. Budzinski, Bruno R. R. Boaretto, Lyle E. Muller, and Ulrike Feudel. Shifts in global network dynamics due to small changes at single nodes. *Physical Review Research*, 5(1):013220, 2023.
- [54] Björn Sandstede. Constructing dynamical systems having homoclinic bifurcation points of codimension two. *Journal of Dynamics and Differential Equations*, 9(2):269–288, 1997.
- [55] Anant Kant Shukla, T R Ramamohan, and S Srinivas. A new analytical approach for limit cycles and quasi-periodic solutions of nonlinear oscillators: the example of the forced Van der Pol Duffing oscillator. *Physica Scripta*, 89(7):075202, 2014.
- [56] W Singer. Neuronal synchrony: a versatile code for the definition of relations? *Neuron*, 24(1):49–65, 1999.
- [57] S. Smale. A Mathematical Model of Two Cells Via Turing’s Equation. In *The Hopf Bifurcation and Its Applications*, pages 354–367. Springer New York, 1976.
- [58] Merten Stender and Norbert Hoffmann. bSTAB: an open-source software for computing the basin stability of multi-stable dynamical systems. *Nonlinear Dynamics*, pages 1–18, 2021.
- [59] Strogatz. *Nonlinear Dynamics and Chaos*. Studies in nonlinearity. Westview, 2002.
- [60] Steven H. Strogatz. From Kuramoto to Crawford: exploring the onset of synchronization in populations of coupled oscillators. *Physica D: Nonlinear Phenomena*, 143(1-4):1–20, 2000.
- [61] Richard Taylor. There is no non-zero stable fixed point for dense networks in the homogeneous Kuramoto model. *Journal of Physics A: Mathematical and Theoretical*, 45(5):055102, 2012.
- [62] Robert L.V. Taylor. Attractors: Nonstrange to Chaotic. *SIAM Undergraduate Research Online*, 4:72–80, 2011. Publisher: Society for Industrial & Applied Mathematics (SIAM).
- [63] Paulo F. C. Tilles, Fernando F. Ferreira, and Hilda A. Cerdeira. Multistable behavior above synchronization in a locally coupled Kuramoto model. *Physical Review E*, 83(6):066206, 2011.
- [64] Emmanuelle Tognoli and J. A.Scott Kelso. The Metastable Brain. *Neuron*, 81(1):35–48, 2014.
- [65] Alex Townsend, Michael Stillman, and Steven H. Strogatz. Dense networks that do not synchronize and sparse ones that do. *Chaos: An Interdisciplinary Journal of Nonlinear Science*, 30(8):083142, 2020.
- [66] D J Watts and S H Strogatz. Collective dynamics of ‘small-world’ networks. *Nature*, 393(6684):440–442, 1998.
- [67] Daniel A. Wiley, Steven H. Strogatz, and Michelle Girvan. The size of the sync basin. *Chaos: An Interdisciplinary Journal of Nonlinear Science*, 16(1):015103, 2006.
- [68] Hugh R. Wilson and Jack D. Cowan. Excitatory and Inhibitory Interactions in Localized Populations of Model Neurons. *Biophysical Journal*, 12(1):1–24, 1972.
- [69] Thilo Womelsdorf and Pascal Fries. The role of neuronal synchronization in selective attention. *Current Opinion in Neurobiology*, 17(2):154–160, 2007.

- [70] Yuanzhao Zhang and Steven H. Strogatz. Basins with Tentacles. *Physical Review Letters*, 127(19):194101, 2021.
- [71] Ronghui Zhu, Jesus M. del Rio-Salgado, Jordi Garcia-Ojalvo, and Michael B. Elowitz. Synthetic multistability in mammalian cells. *Science*, 375(6578):eabg9765, 2022.